
DIGITAL ACCESS TO SCHOLARSHIP AT HARVARD
DASH.HARVARD.EDU


HARVARD LIBRARY
Office for Scholarly Communication

A Clock-Phased Sigma Factor Cascade Is Required for Global Circadian Transcriptional Rhythms in Cyanobacteria

Permanent link
http://nrs.harvard.edu/urn-3:HUL.InstRepos:39987946

Terms of Use
This article was downloaded from Harvard University's DASH repository, and is made available under the terms and conditions applicable to Other Posted Material, as set forth at http://nrs.harvard.edu/urn-3:HUL.InstRepos:dash.current.terms-of-use#LAA

Share Your Story

The Harvard community has made this article openly available.
Please share how this access benefits you. Submit a story .

Accessibility

A Clock-Phased Sigma Factor Cascade is Required for Global Circadian Transcriptional Rhythms in Cyanobacteria

A dissertation presented by
Kathleen Fleming
to
The Department of Molecular and Cellular Biology

in partial fulfillment of the requirements
for the degree of
Doctor of Philosophy
in the subject of
Biology

Harvard University
Cambridge, Massachusetts

July 7th, 2017

© 2017 Kathleen Fleming
All rights reserved.

Dr. Erin O'Shea Kathleen Fleming

A Clock-Phased Sigma Factor Cascade is Required for Global Circadian Transcriptional Rhythms in Cyanobacteria

Abstract

The circadian clock of the cyanobacterium *Synechococcus elongatus* PCC 7942 drives oscillations in global mRNA transcript abundances with 24 h periodicity under continuous light conditions. The transcription factor RpaA controls the timing of circadian gene expression, but the mechanisms underlying RpaA's indirect control of 90-percent of circadian transcripts are not well understood. Here we show that four RpaA-dependent sigma factors – *rpoD2*, *rpoD6*, *rpoD5*, and *sigF2* – are sequentially activated downstream of active RpaA and are required for proper expression of circadian genes. We find that the sigma factors RpoD6, RpoD5, and SigF2 exhibit circadian oscillations with different timing relative to each other at the level of their mRNA expression, protein abundance, and binding enrichment at genomic targets in constant light conditions. We measure global gene expression in strains modified to individually lack *rpoD2*, *rpoD6*, *rpoD5*, and *sigF2*, and identify how expression of circadian genes – including expression of sigma factor genes – is altered in the absence of each sigma factor. Broadly, our findings suggest that a single transcription factor, RpaA, is sufficient to generate complex circadian expression patterns in part by regulating an interdependent sigma factor cascade.

Table of Contents

List of figures and tables

This dissertation is dedicated with love to my aunt Terry Clements.

Introduction

Organisms across different kingdoms of life have evolved anticipatory mechanisms – circadian clocks – that enable coordination of their physiology and behavior with the day-night cycle. Circadian clocks are endogenous 24 h-period oscillators that can keep time for multiple days in constant conditions and can be phase-adjusted to match environmental variation – for example, daily cycling of temperature and light availability (Dunlap et al. 1999; Dunlap 2004; Bell-Pederson el al. 2005). In the simplest model system known to possess a circadian clock, the cyanobacterium *Synechococcus elongatus* PCC 7942, the clock drives daily genome-wide oscillations of mRNA abundances that display a variety of waveforms, amplitudes, and phases (Liu et al., 1995; Golden et al., 1997; Ito et al., 2009; Vijayan et al., 2009). The circadian clock provides *S. elongatus* with competitive advantage when grown in 24 h light-dark cycles (Ouyang et al., 1998; Woelfle et al., 2004). Some of this growth advantage is likely a product of clock-controlled dynamics of gene expression enabling efficient temporal partitioning of biological activities, such as photosynthesis to hours of expected light, and catabolic metabolism pathways (e.g. glycogen degradation, glycolysis, and oxidative pentose phosphate pathway) to hours of expected night (Vijayan et al., 2009; Diamond et al., 2015). The molecular mechanisms underlying the generation of pervasive circadian transcript oscillations are still poorly understood.

The core oscillator in *S. elongatus* is comprised of three proteins (KaiA, KaiB, and KaiC) that sequentially interact to generate circadian (i.e. ~24 h) oscillations in the phosphorylation state of KaiC (Nishiwaki et al., 2007; Rust et al., 2007). Timing information is encoded in the KaiC phosphorylation state and is transduced via two histidine kinases (SasA and CikA) to modulate the phosphorylation state of RpaA, a transcription factor that is required for proper

expression of all circadian genes (Takai et al., 2006; Gutu and O'Shea, 2013; Markson et al., 2013). RpaA phosphorylation and its binding to DNA oscillate in concert with a 24 h period with minimal levels at subjective dawn and maximal levels at subjective dusk (Markson et al., 2013; 'subjective dusk' and 'subjective dawn' refer to an internal estimate of time in the absence of external cues). Remarkably, mimicking the accumulation of active RpaA (RpaA~P) from low levels at subjective dawn to high levels at subjective dusk – by inducing expression of a RpaA phosphomimetic mutant (RpaA-D53E) in cells lacking clock proteins – is sufficient to trigger sequential expression of circadian genes in an order similar to that observed in a natural circadian cycle (Markson et al., 2013). Thus, active RpaA is both necessary and sufficient to transduce information about time of day from the core KaiABC oscillator to circadian gene expression. However, these results do not explain how active RpaA triggers sequential expression of all circadian transcripts as RpaA directly binds upstream of only a small fraction of circadian genes (Markson et al., 2013). RpaA must time the majority of circadian transcript abundances via secondary regulators that function individually or in combination to modulate the synthesis or stability of circadian transcripts.

Top candidates for secondary regulators are four sigma factors – RpoD2, RpoD6, RpoD5, and SigF2 – whose promoters are bound by RpaA and whose expression is altered when RpaA is absent (Markson et al., 2013). Given their RpaA-controlled expression and their predicted roles as global transcriptional activators, these sigma factors could be key regulatory nodes necessary for timing and propagation of the time signal to the entire transcriptome. Across bacterial systems, sigma factors function as transcriptional activators by directing the catalytic core of RNA polymerase to specific transcription start sites and aiding in the initiation of transcription (Felistov et al. 2014). Genomes of many bacterial species, including cyanobacteria, encode

multiple alternative sigma factor genes in addition to a housekeeping sigma factor that directs the bulk of essential gene expression during active growth (Imarua and Asayama 2009). Alternative sigma factors have been implicated in promoting transcription of specialized genes necessary for coping with stress (e.g. iron starvation, nitrogen limitation, reactive oxygen species, temperature, hyperosmolarity, acidic pH) and for driving developmental programs (e.g. endospore formation in *B. subtilis and S. coelicolor*) (Gross et al. 1998; Ishihama 2000; Gruber and Gross 2003). In these examples, the activity of individual sigma factors is temporally controlled by diverse mechanisms including conditional expression of sigma factor transcripts, modulation of sigma factor translation rate, covalent modification of sigma factor proteins, subcellular localization of sigma factor proteins, regulated proteolytic turnover of sigma factor proteins, and sequestration of sigma factor proteins in a manner that abrogates complexing with RNA polymerase (Gruber and Gross 2003). How the eight alternative sigma factor genes encoded in the *S. elongatus* genome are regulated to mediate expression of genes over circadian time or in response to stress has not been systematically determined.

Here we apply biochemical and genetic methods to investigate the roles of the four RpaA-dependent alternative sigma factors RpoD2, RpoD6, RpoD5, and SigF2 in regulating circadian gene expression. We find that protein abundances of RpoD6, RpoD5, and SigF2 and their binding to genomic loci rise and fall in concert with 24 h periodicity and exhibit distinct phasing relative to one another in constant light conditions. Finally, by measuring global gene expression in strains modified to individually lack *rpoD2*, *rpoD6*, *rpoD5*, and *sigF2*, we identify how expression of circadian genes – including expression of the sigma factor genes – are altered in the absence of each sigma factor. Based on our data, we propose that the sigma factor genes *rpoD2*, *rpoD6*, *rpoD5*, and *sigF2* constitute an interdependent and ordered cascade that functions

downstream of active RpaA and forms the basis of a transcriptional network that is required, along with RpaA, to time expression of circadian genes.

Results and Discussion

RpaA-dependent timing of *rpoD2*, *rpoD6*, *rpoD5*, and *sigF2* transcripts and their encoded protein products

Given that *rpoD2*, *rpoD6*, *rpoD5*, and *sigF2* are part of the RpaA regulon and may direct expression of circadian genes downstream of RpaA, we sought to investigate the timing of their expression both at the mRNA and protein level. Transcripts encoding RpoD2, RpoD6, RpoD5, and SigF2 oscillate with 24 h periodicity and exhibit peak expression at different circadian times, with *rpoD2* peaking at T=24 h and 48 h, *rpoD6* peaking at T=32 and 56 h, and both *rpoD5* and *sigF2* peaking at T=36 and 60 h (Figure 1A). Consistent with prior results of Markson et al., we find that sequential changes to *rpoD2*, *rpoD6*, *rpoD5*, and *sigF2* mRNA abundances can be triggered by induction of constitutively active RpaA (phosphomimetic mutant RpaA(D53E)) in cells lacking *kaiBC.* This demonstrates that the sequential timing of sigma factor transcripts is triggered by accumulation of active RpaA downstream of the core KaiABC clock (Figure 1B).

To determine if protein levels of these sigma factors also change over circadian time in a sequential manner that is dependent on RpaA, we measured sigma factor protein levels by immunoblotting over 48 h in constant light (Figure 1A) and over 12 h following induction of constitutively active RpaA in cells lacking *kaiBC* (Figure 1B). To do this, we generated strains in which the sole copy of the respective sigma factor was epitope-tagged and expressed from its native promoter at a neutral locus in the genome. We were able to successfully construct functional, epitope-tagged RpoD6, RpoD5, and SigF2 strains (with functionality assessed by measuring expression of representative circadian genes, including the sigma factor genes; Figure 2), but were unable to generate a functional, epitope-tagged RpoD2 strain. We found that in both in free-running and “active” RpaA induction conditions, RpoD6, RpoD5, and SigF2 protein

levels change over time and peak sequentially with RpoD6 first, then RpoD5, and finally SigF2 (Figure 1A-B, Figure 3, Figure 4). Thus, we conclude that the circadian production of RpoD6, RpoD5, and SigF2 is controlled by RpaA activity, in a manner independent of the KaiABC clock. Notably, for RpoD6, RpoD5, and SigF2 there are differences in the timing of their transcript and protein abundances, revealing that timing of these sigma factor protein levels additionally requires RpaA-dependent translational or post-translational regulation.

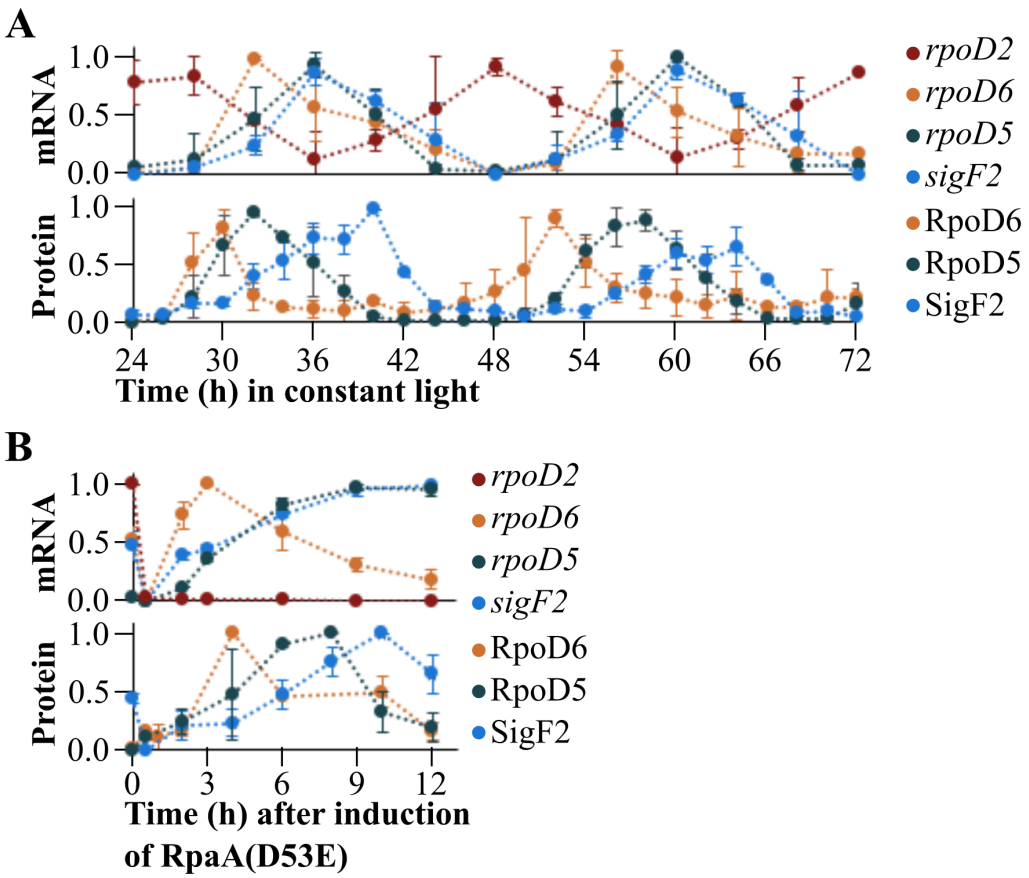

Figure 1. Measurement of *rpoD2*, *rpoD6*, *rpoD5*, and *sigF2* mRNA levels and encoded protein products over time in constant light conditions and following induction of active RpaA in *kaiBC*Δ, *rpaA*Δ, P*trc::rpaA(D53E)* strain.

(A) (Top) Quantification of sigma factor transcript levels in wild-type cells over 48 h, starting at T=24 h after release into constant light. Transcript levels were measured by qRT-PCR and normalized to interval [0 1]; points in the plot represent the mean of three independent experiments with error bars displaying standard deviation. (Bottom) Quantification of sigma factor protein levels over 48 h in epitope-tagged sigma factor strains, starting at T=24 h after release into constant light. Protein levels were measured by immunoblotting and, for each time-series protein, levels were normalized to interval [0 1]; points in the plot represent the mean of three independent experiments with error bars displaying standard deviation.

(B) (Top) Quantification of sigma factor transcript abundances in OX-D53E strain (*kaiBC*Δ, *rpaA*Δ, P*trc::rpaA(D53E);* as described in Markson et al., 2013) before (T=0 h) and after induction of phosphomimetic RpaA by addition of ispropyl-β-D-1-thiogalactopyranoside (IPTG) to 100 μM final concentration. Transcript abundances were measured by RNA-seq and normalized to interval [0 1]; points in the plot represent the mean of two independent experiments with error bar displaying the range. (Bottom) Quantification of sigma factor protein levels in OX-D53E before (T=0 h) and after induction of phosphomimetic RpaA; points in the plot represent the mean of two independent experiments with the error bar displaying the range.

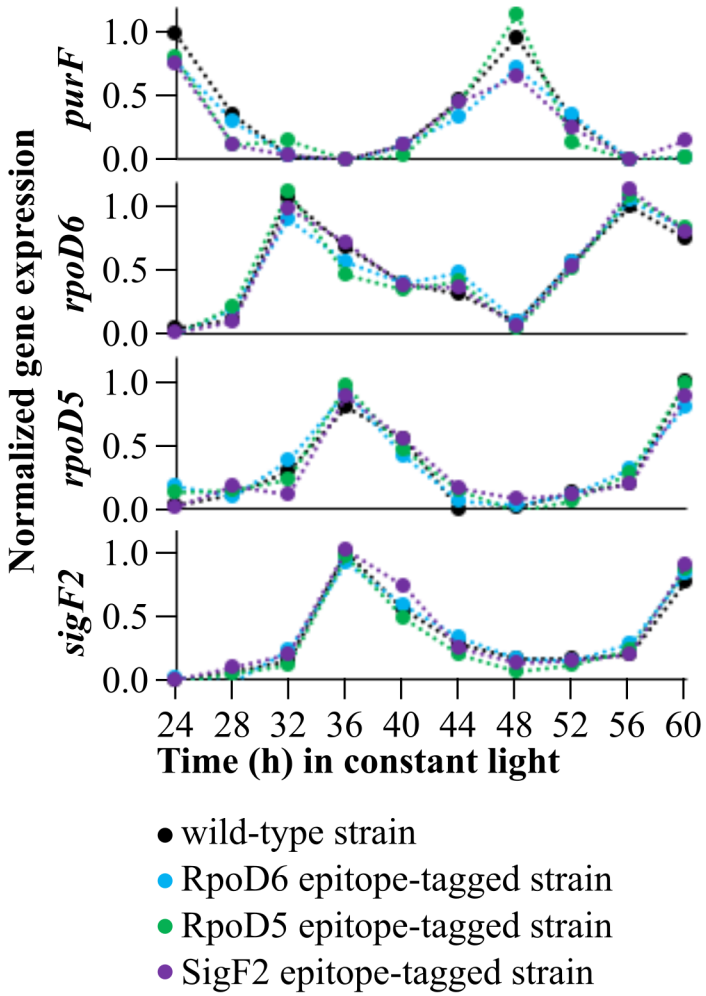

Figure 2. Expression levels of *purF*, *rpoD6*, *rpoD5*, and *sigF2* in the epitope-tagged sigma factor strains over time in constant light conditions.
Quantification of transcript levels in wild-type and sigma factor epitope-tagged strains over 36 h, starting at T=24 h after release into constant light. Transcript abundances were measured by qRT-PCR and normalized relative to the minimum and maximum values measured in the wild-type strain.

Figure 3. Measurement of RpoD6, RpoD5, and SigF2 protein levels over time in constant light. Western blots for measuring sigma factor protein levels over 48 h, starting at T=24 h after release into constant light in epitope-tagged sigma factor strains; (A) RpoD6, (B) RpoD5, and (C) SigF2. Equal total protein content for each lysate, as determined by Bradford assay, was loaded to each lane; duplicate gels stained with Coomassie dye served as a loading controls. An example of a Coommassie stained gel for one of the replicate time-series is shown.

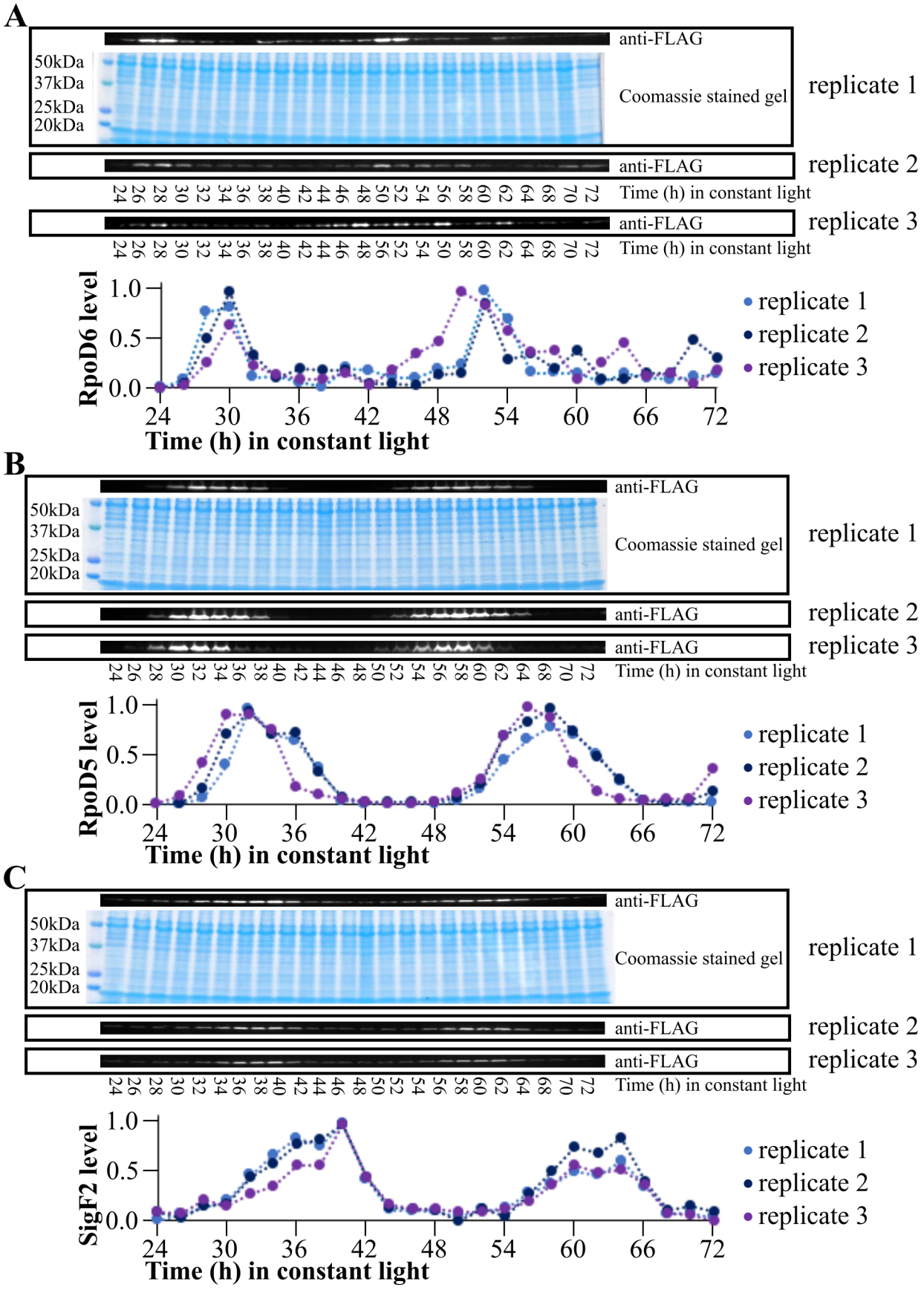

Figure 3 (Continued).

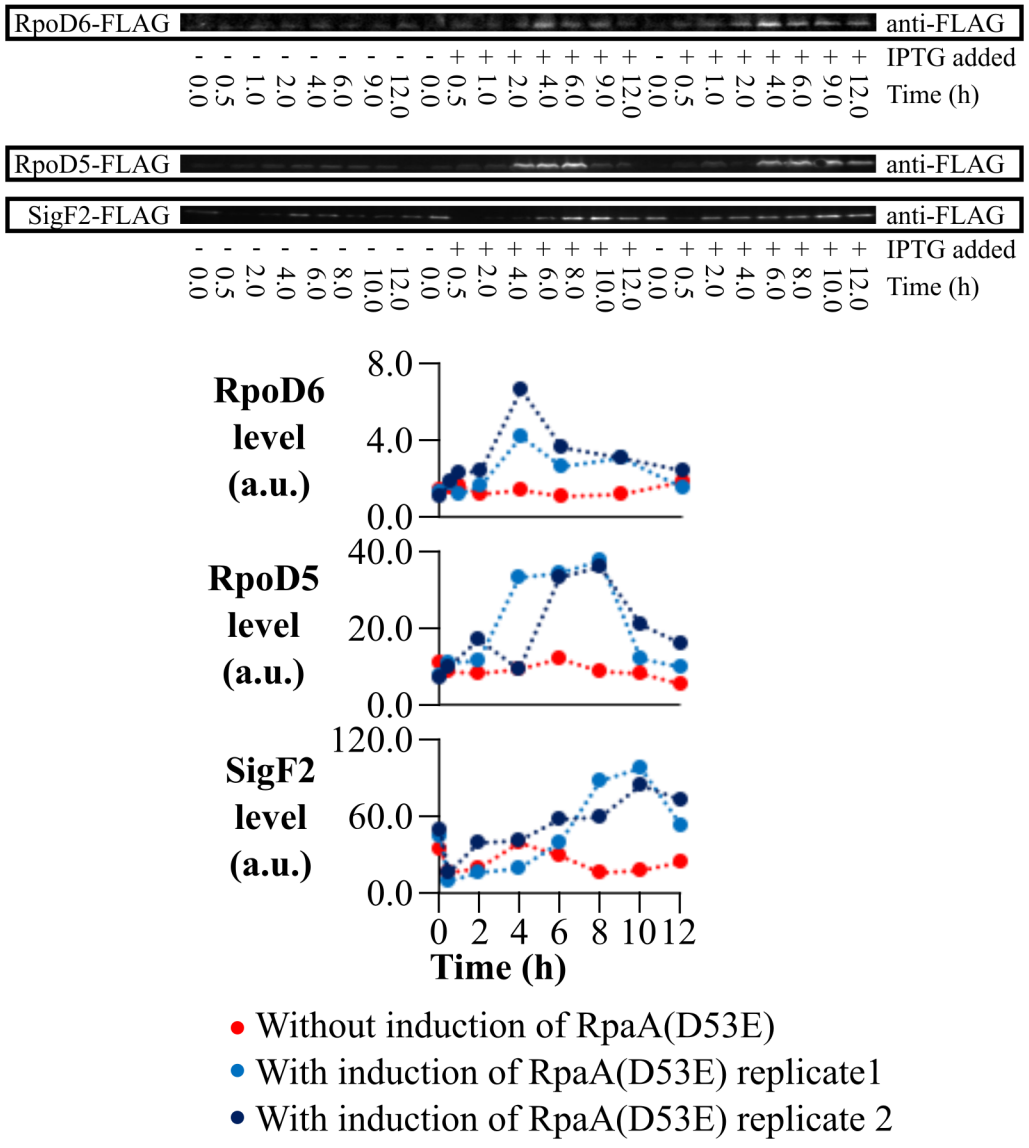

Figure 4. Measurement of RpoD6, RpoD5, and SigF2 protein levels before and after induction of active RpaA in *kaiBC*Δ, *rpaA*Δ, *Ptrc::rpaA(D53E)* strain.
Western blots for measuring sigma factor protein levels in OX-D53E strains modified to have the sole copy of the sigma factor epitope-tagged and expressed from native promoter at a neutral locus in the genome before (T=0 h) and after induction of phosphomimetic RpaA by addition of IPTG to 100 μM final concentration. Equal total protein content for each lysate, as determined by Bradford assay, was loaded to each lane.

ChIP-seq reveals the landscape of RpoD6, RpoD5, and SigF2 binding upstream of transcription start sites for circadian genes

If sigma factors compete for association with the core RNA polymerase, and if different forms of RNA polymerase holoenzymes can recognize *S. elongatus* promoters, we predict that RpoD6, RpoD5, and SigF2 will bind circadian promoter targets maximally at different times of day. To identify RpoD6, RpoD5, and SigF2 binding sites at a genome-wide level and characterize the dynamics of their binding over time, we utilized our functional, epitope-tagged sigma factor strains to perform circadian time course chromatin immunoprecipitation, analyzed by high-throughput sequencing (ChIP-seq), for each sigma factor every 4 h over 48 h in constant light conditions. To make initial assignments of sigma factor binding sites to specific transcripts, we first determined the locations of transcription start sites genome-wide. To do this, we utilized a functional, epitope-tagged RNA polymerase strain (gift of A. Puszynska, Harvard University) to perform circadian time course ChIP-seq on cells treated with rifampicin to lock RNA polymerase at initiation sites genome-wide (Supplementary Table 1; see Experimental Procedures). We focused our analysis on high-confidence circadian genes (n=336), a subset of the circadian genes defined by Markson et al. that have greater than 1.75 ratio of peak to trough expression in wild-type cells grown in constant light conditions, and have a transcription start site within 250 base pairs upstream of their start codon. We find that RpoD6, RpoD5, and SigF2 bind upstream of transcription start sites for circadian genes maximally at different times of day: RpoD6 at T=28 and 52 h, RpoD5 at T=32/36 and 56/60 h, and SigF2 at T=40 and 64 h (Figure 5A, Supplementary Tables 2-4). Furthermore, these three sigma factors bind their promoter targets maximally when their protein abundance is also maximal, consistent with a model of sigma factors competing to bind RNA polymerase, which could time the transcription of

different circadian genes. We note also that RpoD6, RpoD5, and SigF2 all bind their own promoters as well as promoters of other sigma factors. For instance, RpoD6 binds the promoter of *rpoD5* and RpoD5 binds the promoter of *rpoD6*, which suggest presence of auto- and cross-regulatory feedback mechanisms. In total, we determined that 132 of the 336 high-confidence circadian transcripts (40-percent) are bound by RpoD6, RpoD5, or SigF2, and 41 of 132 are bound by more than one sigma factor (Figure 5B). Intriguingly, the circadian promoter targets of a given sigma factor are not expressed with a similar phase (Figure 5A), suggesting that there are additional factors directing the timing of peak transcript abundances.

Consistent with the possibility that RpoD6, RpoD5, and SigF2 could control other genes whose product can modulate gene expression, we find three transcription factors (*synpcc7942_0090*, *synpcc7942_0556*, and *sypncc7942_1159*) and three sigma factors (*rpoD1*, *rpoD3*, and *rpoD4*) as members of their putative regulons. RpoD6 binds the promoters of *synpcc7942_0090, synpcc7942_0556, rpoD1,* and *rpoD4.* RpoD5 binds the promoters of *synpcc7942_0090, synpcc7942_0556, sypncc7942_1159, rpoD3,* and *rpoD4.* Given that transcript abundances of these transcription factors and sigma factors exhibit circadian oscillations, these factors may act like RpoD6, RpoD5, and SigF2 to compete to complex with RNA polymerase, bind circadian promoters at specific times of day, and contribute to circadian timing of specific transcript abundances.

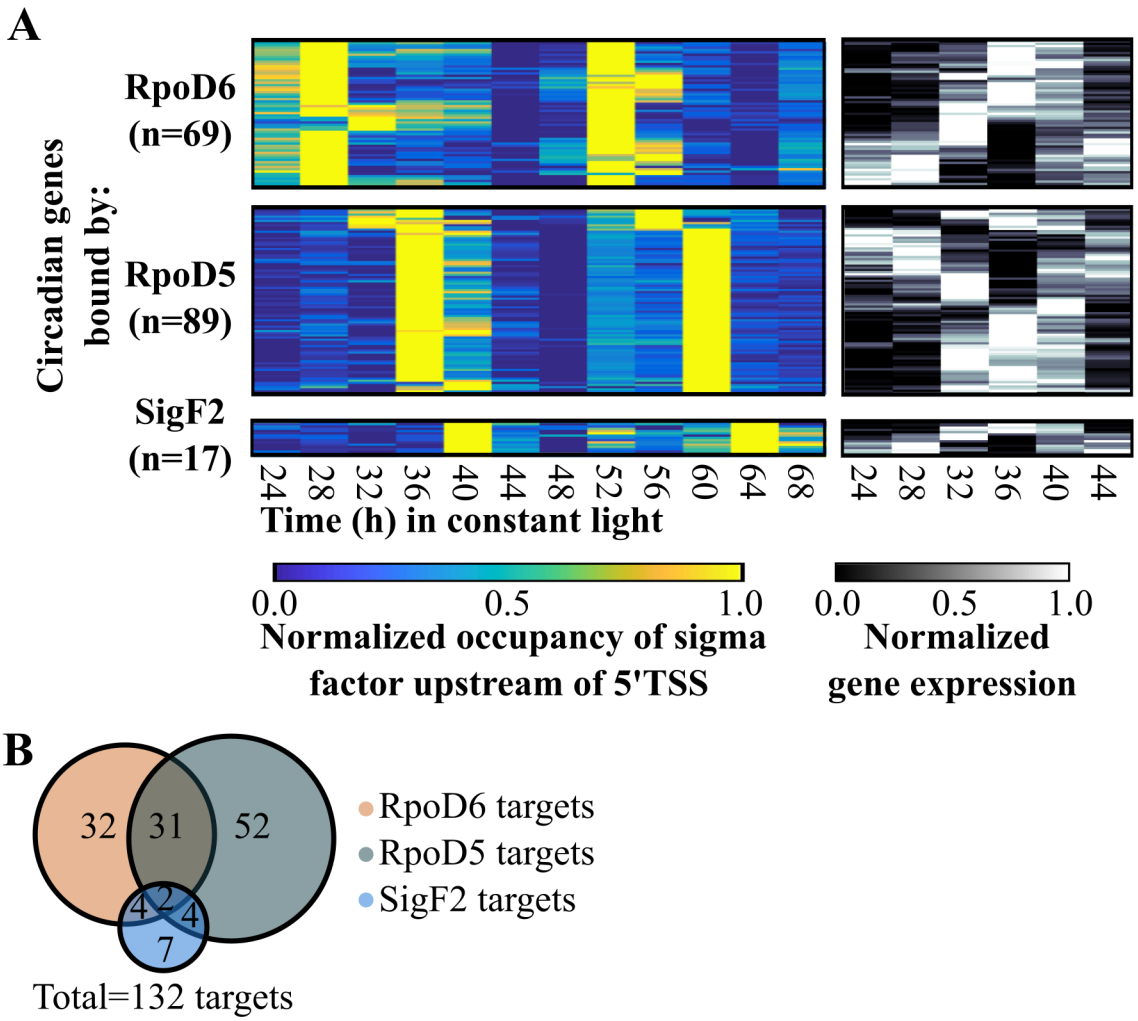

Figure 5. Dynamics of RpoD6, RpoD5, and SigF2 enrichment upstream of transcription start sites (TSS) of circadian transcripts over time.
(A) ChIP-Seq was performed every 4 h for 48 h starting at T=24 h after release into constant light. Enrichment relative to the mock IP was calculated at the location of maximum ChIP-Seq read density within each binding site. (Left) Each row in the heatmaps represents the enrichment relative to the mock immunoprecipitation, normalized to interval [0 1]. (Right) Transcript abundance in wild-type cells of mRNAs encoded immediately downstream of each circadian promoter target shown on the left, over 24 h after release into constant light. Transcript abundances were normalized to interval [0 1].
(B) Venn diagram displaying overlap of circadian targets bound by RpoD6, RpoD5, and SigF2.

***rpoD2*, *rpoD6*, *rpoD5*, and *sigF2* are required for proper expression of circadian genes**

To determine whether the sigma factors RpoD2, RpoD6, RpoD5, and SigF2 are required for proper expression of circadian transcripts, we sought to investigate if and how inactivation of individual sigma factor genes altered expression of circadian genes. Previously, Nair et al. deleted *rpoD2* and *rpoD5* in a P*kaiBC::luxAB* reporter strain and found that inactivation of *rpoD2* increased the period of P*kaiBC::luxAB* expression with no effect on amplitude, while inactivation of *rpoD5* decreased the amplitude of P*kaiBC::luxAB* expression with no affect on period length (Nair et al., 2002). Given that changes in the expression of *kai* proteins can perturb Kai protein stoichiometry and disrupt KaiABC clock function (Takai et al., 2006; Markson et al., 2013), it is possible that KaiABC clock function is disrupted or altered in cells singly lacking *rpoD2* or *rpoD5*. To avoid secondary affects to gene expression that might arise if there exists sufficient disruptive feedback from sigma factor genes to KaiABC clock function or RpaA regulation, we prioritized deleting sigma factor genes in the OX-D53E strain that has upstream KaiABC and RpaA regulation genetically abolished and has RpaA-dependent gene expression output artificially restored (OX-D53E strain: *kaiBC*Δ*, rpaA*Δ*, Ptrc::rpaA(D53E)*, as we used for Figure 1B). We generated deletion strains of *rpoD2*, *rpoD6*, and *rpoD5* in the OX-D53E background. Despite our repeated attempts, we were unable to generate a complete deletion of *sigF2* in this background, and therefore generated the *sigF2* deletion in a wild-type background only. After confirming that induction of active RpaA or its phosphorylation profile remained unaffected in the sigma deletion strains (Figure 6, Figure 7), we analyzed by RNA-seq the kinetics and peak levels of mRNA accumulation following induction of RpaAD53E in *rpoD2*, *rpoD6*, *rpoD5* deletion strains (Figure 8A), and overall transcriptome changes in the *sigF2* deletion strain (Figure 8B). We find that individual inactivation of *rpoD2*, *rpoD6*, *rpoD5*, and

sigF2 (in the wild type background) alters temporal transcript levels and peak abundance for some circadian genes and not others.

Figure 6. Induction of RpaA(D53) expression in strains individually lacking *rpoD2*, *rpoD6*, and *rpoD5.*
(A) Western blot analysis of phosphomimetic RpaA protein levels before (T=0 h) and after induction of phosphomimetic RpaA by addition of IPTG to 100 μM final concentration in OX-D53E strain, OX-D53E strain lacking *rpoD2*, OX-D53E strain lacking *rpoD6*, and OX-D53E strain lacking *rpoD5*. RpaA(D53E) protein levels over time in each strain were normalized to interval [0 1]. Equal total protein content for each lysate, as determined by Bradford assay, was loaded to each lane.
(B) Western blot analysis comparing the abundance of RpaA(D53E) at T=12 h after induction of phosphomimetic RpaA for replicate 1 of all strains shown in (A). Equal total protein content for each lysate, as determined by Bradford assay, was loaded to each lane.

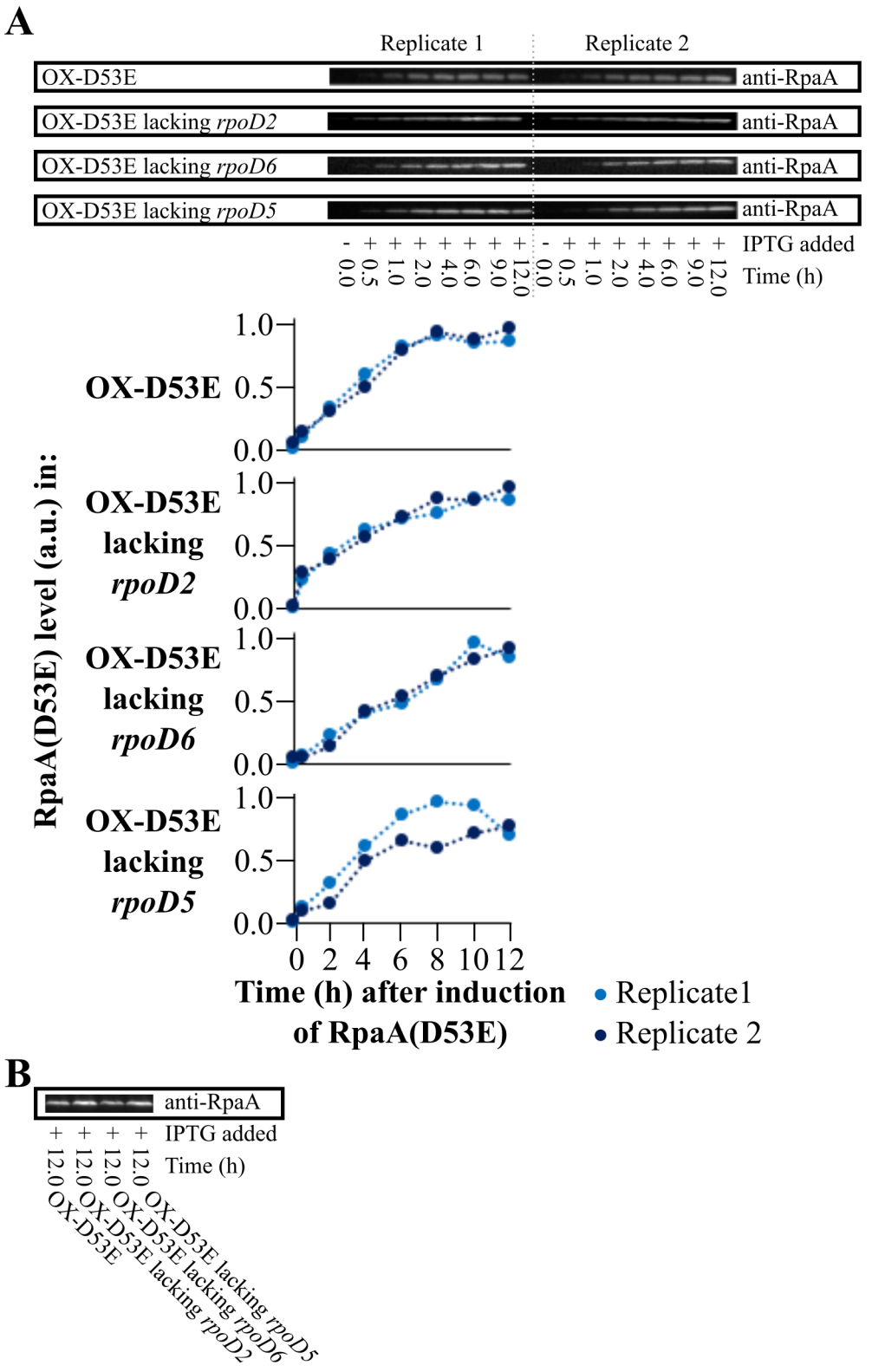

Figure 6 (Continued.)

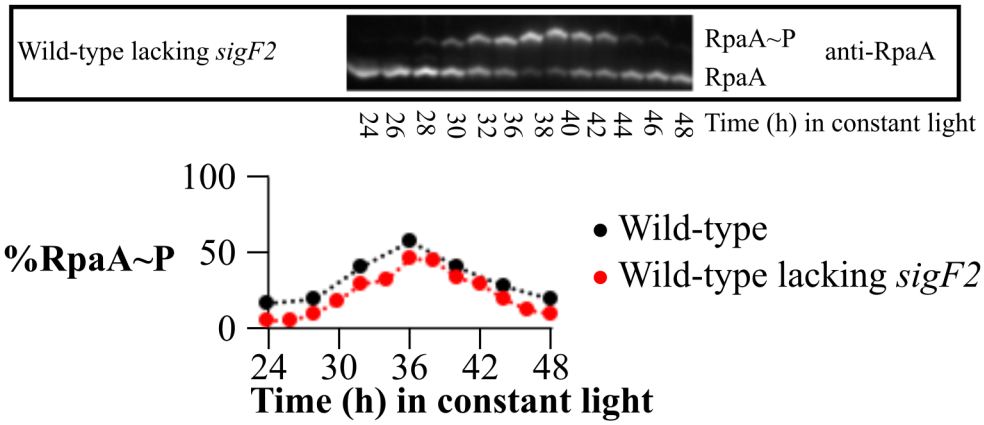

Figure 7. Levels of phosphorylated RpaA protein in the wild-type strain lacking *sigF2* over time in constant light assessed by Phos-tag western blotting.
(Top) Phos-tag western blot of phosphorylated and unphosphorylated RpaA over time. Lysates were prepared from wild-type cells lacking *sigF2* and equal total protein content for each lysate, as determined by Bradford assay, was loaded to each lane.
(Bottom) Quantification of RpaA~P levels over 24 h in constant light in the wild-type strain lacking *sigF2* (red) compared to levels in wild-type strain (black; data from Markson et al., 2013).

Figure 8. Expression of circadian genes in strains individually lacking *rpoD2*, *rpoD6*, *rpoD5*, and *sigF2*.
(A) Time courses of transcript levels for circadian genes (n=336) in OX-D53E strain and in OX-D53E strains modified to lack individual sigma factor genes *rpoD2*, *rpoD6*, and *rpoD5*. Gene expression was measured by RNA-seq before (T=0 h) and after induction of phosphomimetic RpaA in two independent experiments for each strain. Mean time-series transcript levels for each strain were normalized to the interval [0 1] and sorted based on peak expression in wild-type cells (see panel B). To compare how the peak transcript abundance of each circadian gene is changed in the sigma factor deletion strain relative to the OX-D53E strain, the ratio is displayed as a colored row normalized to interval [0.3 3.0], reflecting ≥3-fold reduction and ≥3-fold increase respectively in peak transcript abundance in the sigma factor deletion strain.
(B) Time courses of transcript levels for circadian genes (n= 336) in wild-type strain and in a wild-type strain modified to lack the *sigF2* gene. Gene expression was measured by RNA-seq over one circadian cycle in two independent experiments for each strain starting at T=24 h after release into constant conditions. Mean time-series transcript levels for each strain were normalized to the interval [0 1] and sorted based on peak expression in wild-type cells. To compare how the peak transcript abundance of each circadian gene is changed in the *sigF2* deletion strain relative to the wild-type strain, the ratio is displayed as a colored row normalized to interval [0.3 3.0], reflecting ≥3-fold reduction and ≥3-fold increase respectively in peak transcript abundance in the *sigF2* deletion strain.

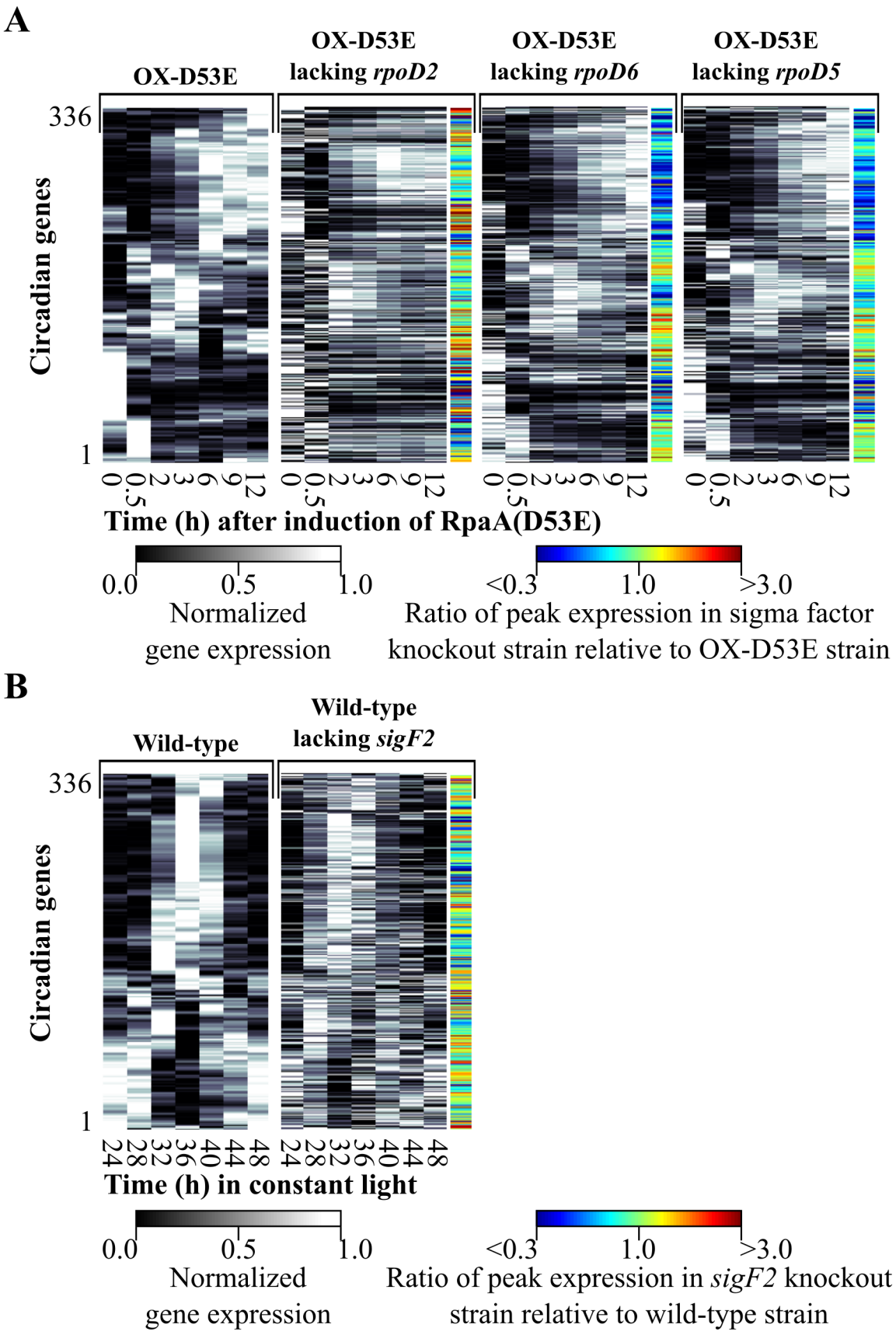

Figure 8 (Continued).

To compare how transcript levels for circadian genes are altered across sigma factor deletion strains, we generated a heatmap based on two metrics for each circadian gene in the four sigma factor deletion strains. The first metric is the cross-correlation value of the time-series transcript levels, normalized to the interval [0 1], in the sigma factor deletion strain compared to in the reference strain (e.g. transcript levels in the OX-D53E strain lacking *rpoD2* compared to the OX-D53E strain). This value ranges from -1 reflecting a strong negative correlation to +1 reflecting a strong positive correlation. The second metric is the ratio of peak expression in the sigma factor deletion strain compared to peak expression in the reference strain. Together the two metrics describe how timing of transcript levels and peak expression are altered for each circadian gene. The heatmap we generated based on these two metrics for each sigma factor deletion strain reveals that transcript levels for some circadian genes are altered differently depending on which sigma factor is inactivated, while transcript levels of other circadian genes are altered similarly in two or more sigma factor deletion strains (Figure 9). For example, cluster I in Figure 9 contains circadian genes for which transcript timing is not altered in cells lacking *rpoD6*, *rpoD5*, or *sigF2*, but in cells lacking *rpoD2* the transcript level timing is altered and peak expression is elevated. In contrast, cluster II in Figure 9 contains circadian genes for which transcript timing is similar in the cells individually lacking the four sigma factors, but transcript peak expression is altered to different extents depending on which sigma factor is inactivated with similar reductions often observed in cells lacking *rpoD6* and in cells lacking *rpoD5*. As one final example, cluster III in Figure 9 contains circadian genes for which transcript timing is similar in cells lacking *rpoD6*, *rpoD5*, or *sigF2,* but in cells lacking *rpoD2* the transcript level timing is altered and peak expression is repressed. These complex alterations to the expression of circadian genes are inconsistent with a simple model in which the sigma factors function

independently of one another to modulate circadian gene expression. Instead, the function of the sigma factors must be required interdependently for proper gene expression.

Our data reveals that interdependence amongst the sigma factors is partially set at the level of sigma factor expression. For example, in OX-D53E cells lacking *rpoD6* we observed unperturbed *rpoD2* levels and constitutively low levels of *rpoD5* and *sigF2* (Figure 10A). This is consistent with *rpoD6* acting downstream of *rpoD2* and upstream of *rpoD5* and *sigF2* by activating their expression. In OX-D53E cells lacking *rpoD5* we observed unperturbed *rpoD2* levels, constitutively low levels of *sigF2*, and *rpoD6* levels that remain elevated at later times (Figure 10A). This is consistent with *rpoD5* acting downstream of *rpoD2* to activate *sigF2* expression and to repress *rpoD6* expression. In OX-D53E cells lacking *rpoD2* we observed that *sigF2* levels were six-fold upregulated at T=0 h prior to induction of active RpaA and following induction *rpoD6*, *rpoD5*, and *sigF2* levels increased, but with altered temporal profiles – the kinetics of *rpoD6* reducing in level are altered and both *rpoD5* and *sigF2* levels increase by T=12 h, but exhibit peak expression that is reduced two-fold. (Figure 10A). This is consistent with *rpoD2* levels being required at subjective dawn (when RpaA activity is at minimum) to repress *sigF2* and RpaA-dependent early repression of *rpoD2* being required upstream of changes to *rpoD6*, *rpoD5*, and *sigF2* levels. To test if constitutively high levels of *rpoD2* are sufficient to block activation of *rpoD6*, *rpoD5*, and *sigF2* levels, we replaced the native promoter region of *rpoD2* with a constitutive promoter (*PSynpcc7942_0456*) that is not dependent on RpaA activity and measured by qRT-PCR the changes in *rpoD6*, *rpoD5*, and *sigF2* transcript levels following induction of RpaAD53E. In cells with constitutive *rpoD2* expression we observed constitutively low levels of *rpoD6*, *rpoD5*, and *sigF2* (Figure 10A). This pattern of regulation is consistent with RpaA-dependent reduction of *rpoD2* levels being required to relieve *rpoD2*-dependent repression of downstream sigma factors *rpoD6*, *rpoD5*, and *sigF2*. In total, the

observed dependencies amongst the sigma factors include: *rpoD2*-dependent repression of *rpoD6*, *rpoD5*, and *sigF2*, *rpoD6*-dependent activation of *rpoD5* and *sigF2*, *rpoD5*-dependent repression of *rpoD6*, and *rpoD5*-dependent activation of *sigF2*. Based on these genetic interactions we propose that *rpoD2*, *rpoD6*, *rpoD5*, and *sigF2* constitute an interdependent and ordered cascade that is triggered by RpaA-dependent repression of *rpoD2* (Figure 10B). We further propose that this sigma factor network is required with active RpaA to properly time expression of circadian genes between subjective dawn and subjective dusk. The only inferred relationship that is potentially direct is the binding of RpoD6 to activate *rpoD5* expression, as we found that RpoD6 binds upstream of *rpoD5*. Potentially the *rpoD5*-dependent activation of *sigF2* expression, while not mediated by RpoD5 binding, could be mediated by *synpcc7942_0090, sypncc7942_1159, rpoD4,* or *sypncc7942_1108* all of which are bound by RpoD5, exhibit reduced expression in cells lacking *rpoD5,* and encode proteins that are predicted to modulate transcription (i.e. transcription factor, sigma factor, nucleoid associated protein).

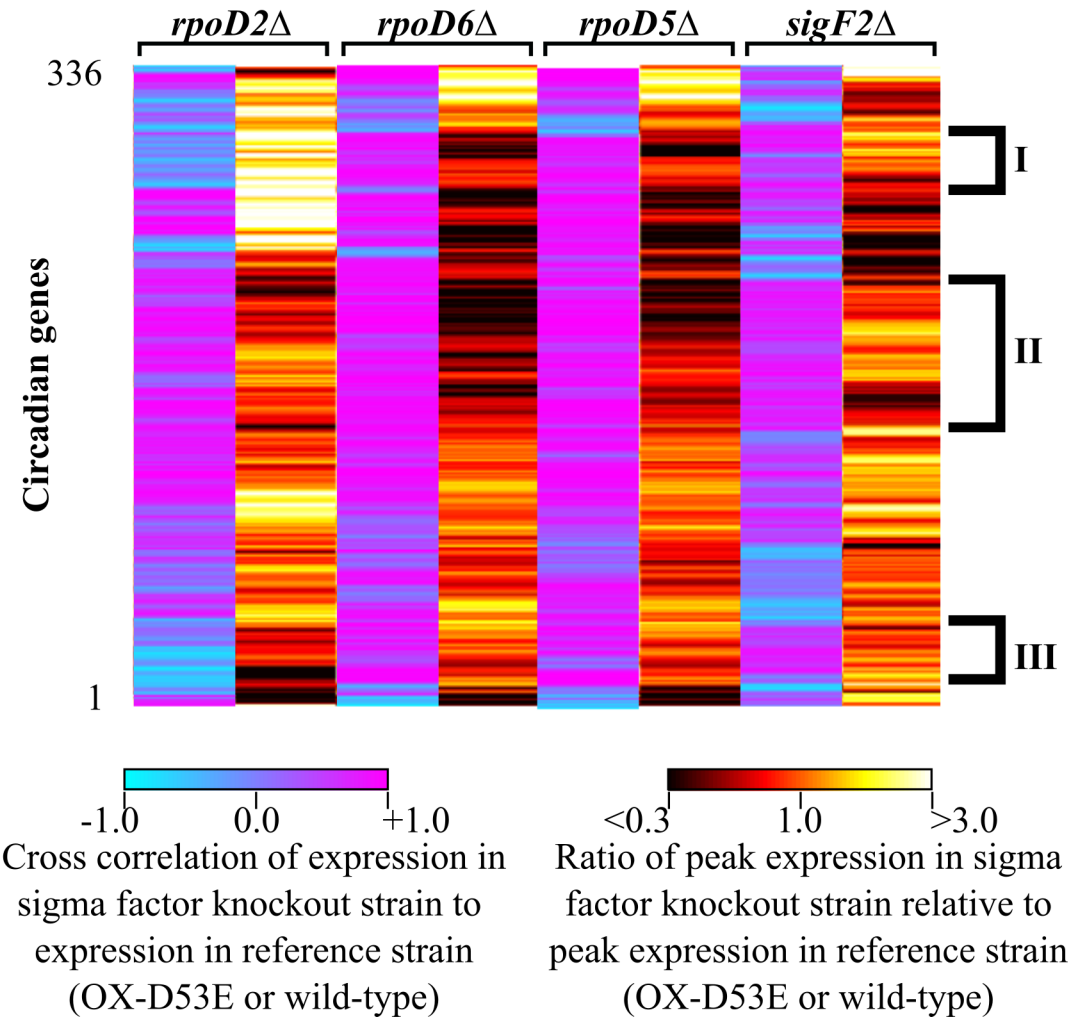

Figure 9. Heatmap showing how timing and peak expression of circadian transcripts are altered in the absence of *rpoD2*, *rpoD6*, *rpoD5*, and *sigF2*.
The heatmap was generated based on two metrics calculated for each circadian transcript based on data shown in Figure 9. The first metric is the cross-correlation value of the time-series transcript levels normalized to interval [0 1] in the sigma factor deletion strain compared to in the reference strain (e.g. transcript levels in the OX-D53E strain lacking *rpoD2* compared to the OX-D53E strain); this value ranges from -1 reflecting a strong negative correlation to +1 reflecting a strong positive correlation. The second metric is the ratio of peak expression in the sigma factor deletion strain compared to peak expression in the reference strain; the ratio is displayed normalized to interval [0.3 3.0], reflecting ≥3-fold reduction and ≥3-fold increase respectively in peak transcript abundance in the sigma factor deletion strain. Together the two metrics describe how timing of transcript levels and peak expression are altered for each circadian gene. The heatmap rows were ordered based on hierarchical clustering that sought to minimize Euclidean distance.

Figure 10. Alterations to sigma transcript levels in sigma factor knockout strains reveal dependencies amongst the sigma factors.
(A) RpaAD53E-induced dynamics of *rpoD2*, *rpoD6*, *rpoD5*, and *sigF2* mRNA levels before (T=0 h) and after induction of phosphomimetic mutant RpaA (RpaA(D53E)) in the OX-D53E strain, OX-D53E strain lacking *rpoD6*, OX-D53E strain lacking *rpoD5*, OX-D53E strain lacking *rpoD2*, and OX-D53E strain with *PrpoD2* replaced by *Psynpcc7942_0456*. Transcript levels of *rpoD2*, *rpoD6*, *rpoD5*, and *sigF2* were measured by RNA-seq and are shown normalized to the interval [0 1,] with 0 and 1 reflecting the minimum and maximum expression in the OX-D53E strain respectively; points in the plot represent the mean of two independent experiments. For the OX-D53E strain with *PrpoD2* replaced by *Psynpcc7942_0456* transcript levels were measured by qRT-PCR; points in the plot represent the mean of two independent experiments.
(B) Diagram reflects the synthesis of genetic interactions between the sigma factor genes *rpoD2*, *rpoD6*, *rpoD5*, and *sigF2* inferred from data displayed in (A).

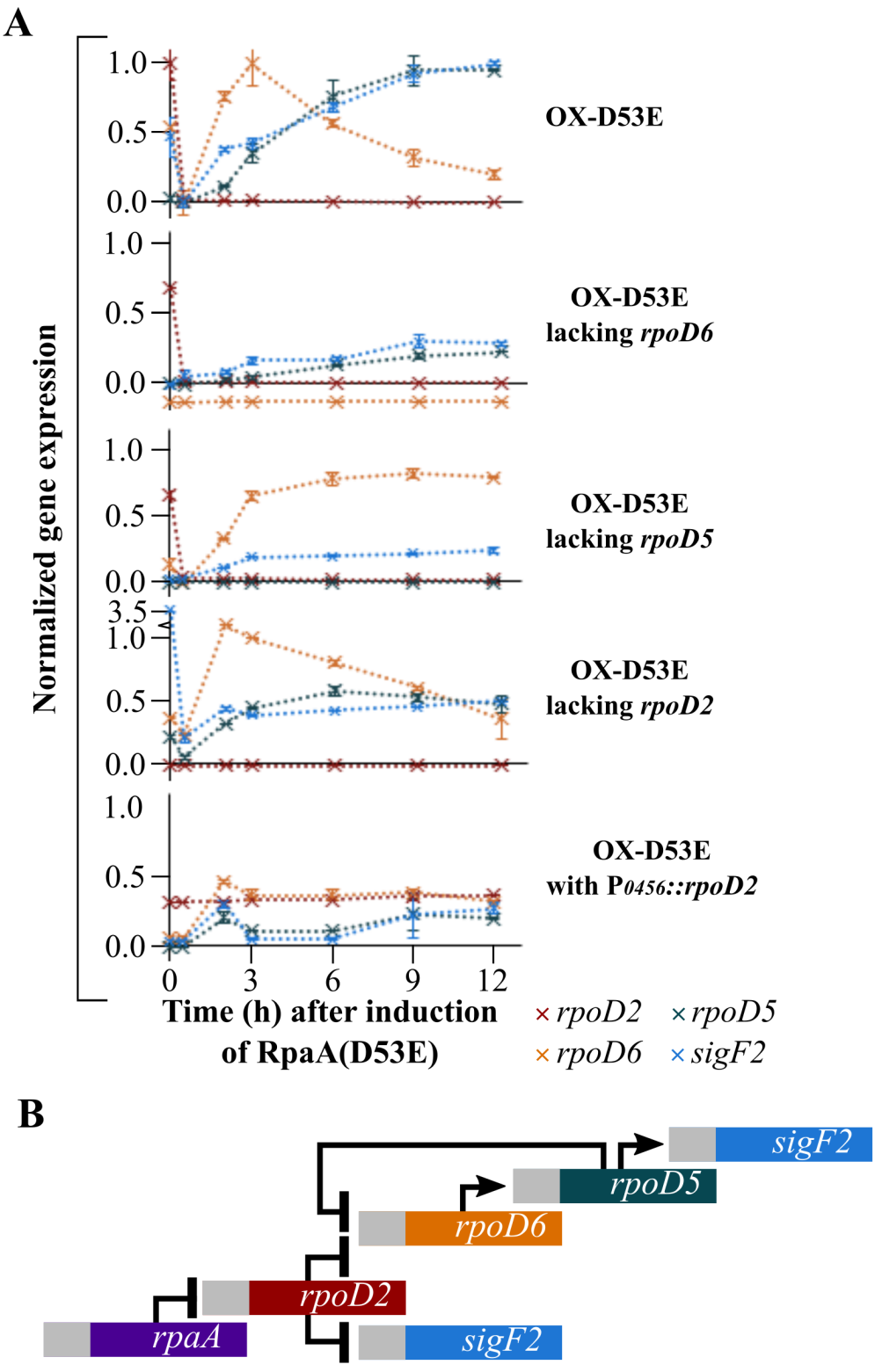

Figure 11 (Continued).

Concluding remarks

RpaA is a master transcriptional regulator, required for proper expression of all circadian genes. In this study, we demonstrate that RpaA times circadian gene expression in part via the alternative sigma factors *rpoD2*, *rpoD6*, *rpoD5*, and *sigF2*. Our core finding is that individual inactivation of *rpoD2*, *rpoD6*, *rpoD5*, or *sigF2* alters the timing and peak expression of some circadian genes downstream of active RpaA, while the expression of other circadian genes is unaffected (Figure 8). The expression changes that we observe in the different sigma factor deletion strains (Figure 9) suggest that the sigma factors *rpoD2*, *rpoD6*, *rpoD5*, and *sigF2* function interdependently to affect mRNA abundances of circadian genes downstream of active RpaA accumulation (Figure 10). Notably, our data reveals that the sigma factor interdependence is at least partially set at the level of sigma factor expression, as deletion of a sigma factor (e.g. *rpoD6*) alters the transcript levels of other sigma factors (e.g. *rpoD5* and *sigF2*). In total, the genetic interactions among the sigma factors that we observe are consistent with the sigma factors *rpoD2*, *rpoD6*, *rpoD5*, and *sigF2* constituting an ordered cascade (Figure 10B) that is triggered by RpaA-dependent repression of *rpoD2*. Given that we observe expression defects when the timing and peak abundance of *rpoD2*, *rpoD6*, *rpoD5*, and/or *sigF2* transcripts are disrupted (Figure 8), these sigma factor genes must at least partially underlie the generation of global circadian gene expression in this cyanobacterium.

How the sigma factors RpoD2, RpoD6, RpoD5, and SigF2 directly and indirectly contribute to waveforms, amplitudes, and phasing of circadian transcripts remains unclear. We did find that RpoD6, RpoD5, and SigF2 protein abundances and occupancy upstream of target circadian genes changes over circadian time with distinct phasing relative to one another. Based on this, we propose that directed changes to pools of sigma factor species over circadian time and sigma

factors competing to recruit RNA polymerase to specific genomic regions could contribute to transcript synthesis rates for specific circadian genes. Direct measurement of sigma factors complexing with RNA polymerase over circadian time and of genome-wide nascent RNA levels generated by distinct sigma factor/RNA polymerase holoenzymes relative to those generated by all species of RNA polymerase holoenzymes will determine if basic tenets of this model are correct.

Also meriting future investigation is the timing of *rpoD2*, *rpoD6*, *rpoD5*, and *sigF2* transcript levels. How are transcript abundances of these sigma factors reproducibly and sequentially timed downstream of active RpaA? The interdependencies among the sigma factors that we elucidated (Figure 10B) may guarantee the ordering of their peak transcript abundances, but are alone unlikely to control the reproducible time intervals between their activations that we observe in constant light conditions (Figure 1A). Potentially, the time intervals between sigma factor peak transcript abundances are tied to the dynamics of active RpaA accumulation. This coupling would ensure that the sigma factor cascade remains synchronized with time of day information stored in the KaiABC clock. A potential mechanism for this could be the combination of sigma factor expression being driven by different levels of active RpaA, and RpaA's transcriptional activity at promoters of r*poD6*, *rpoD5*, and *sigF2* requiring outputs generated by earlier sigma factors (e.g. *rpoD5*-dependent output needed with RpaA binding at a threshold level of active RpaA to activate *sigF2* expression). Said another way, each step of the sigma factor cascade could require both completion of the previous cascade stage and a threshold level of active RpaA. This 'AND' gate model predicts that different dynamics of RpaA phosphorylation over 24 h will alter the timing between sigma factors (e.g. delaying or accelerating transitions) without changing the cascade sequence. Additionally, this model predicts that natural environmental

variations (e.g. changes in light intensity) that transiently or reversibly alter RpaA action – such as those predicted to be mediated by the response regulator RpaB (Espinosa et al., 2015) – may be sufficient to transiently stall progression of the sigma factor cascade. This model could be tested either by altering the dynamics of active RpaA accumulation in OX-D53 cells (e.g. by adding different concentrations of IPTG inducer) or by abrogating RpaA binding at specific sigma factor promoters in OX-D53E cells (e.g. replacing the RpaA consensus motif upstream of sigma factor transcription start sites with a scrambled DNA sequence). The former test would be predicted to change the relative timing between sigma factor transcript activations with the rate of active RpaA accumulation correlating inversely with time delays between peak expression of *rpoD2*/*rpoD6* and *rpoD6*/*rpoD5*. The latter test would be predicted to prevent the activation of downstream sigma factors, thus stalling progression of the sigma factor cascade.

Experimental Procedures

Plasmid construction

All plasmids for strain construction were generated using Gibson assembly (Gibson et al., 2009) and verified by Sanger sequencing.

i. The KF-P-05 plasmid was constructed by insertion of DNA sequence for P*rpoD5*::*rpoD5*-GSGS-3XFLAG$_C$ into the XhoI site of the NS2.2 (Gm^R; gentamicin resistance) targeting vector. The DNA sequence for P*rpoD5*::*rpoD5*-GSGS-3XFLAG$_C$ was generated by a series of nested PCR reactions. The P*rpoD5* was taken as 600 base pairs of sequence located upstream of the *rpoD5* translation start codon (ATCC PCC 7942 chromosomal sequence 1916020 to 1916619 bps). The *rpoD5*-GSGS-3XFLAG$_C$ was generated by appending the coding sequence of *rpoD5* (chromosomal sequence 1916620 to 191781 bps) to the DNA sequence for the GSGS-3XFLAG epitope tag (GGCAGCGGCA GCGATTACAA AGATCACGAT GGCGATTACA AAGATCACGA TATCGATTAC AAAGATGATG ATGATAAA) which itself was appended to the DNA sequence for a stop codon (TAG).

ii. The KF-P-13 plasmid was constructed by insertion of P*rpoD5*::*rpoD5*-GSGS-3XFLAG$_C$ sequence from KF-P-05 into SalI site of the NS1 (Sp^R; spectinomycin resistance) targeting vector (pAM1303, gift of Dr. Susan Golden, University of California, San Diego).

iii. The KF-P-06 plasmid was constructed by insertion of DNA sequence for P*rpoD6*::*rpoD6*-GSGS-3XFLAG$_C$ into XhoI site of the NS2.2 (Gm^R; gentamicin resistance) targeting vector. The DNA sequence for P*rpoD6*::*rpoD6*-GSGS-3XFLAG$_C$ was generated by a series of nested PCR reactions. The P*rpoD6* was taken as the 600 base pairs of sequence located upstream of the *rpoD6* translation start codon (reverse complement of chromosomal sequence 1614397-1614996 bps). The *rpoD6*-GSGS-3XFLAG$_C$ was generated by appending the coding sequence

of *rpoD6* (reverse complement of chromosomal sequence 1613467 to 1614396 bps) to the DNA sequence for the GSGS-3XFLAG epitope tag (GGCAGCGGCA GCGATTACAA AGATCACGAT GGCGATTACA AAGATCACGA TATCGATTAC AAAGATGATG ATGATAAA) which itself was appended to the DNA sequence for a stop codon (TAG).

iv. The KF-P-14 plasmid was constructed by insertion of P*rpoD6*::*rpoD6*-GSGS-3XFLAG$_C$ sequence from KF-P-06 into SalI site of the NS1 (Sp^R; spectinomycin resistance) targeting vector (pAM1303).

v. The KF-P-08 plasmid was constructed by insertion of DNA sequence for P*sigF2*::*sigF2*-GSGS-3XFLAG$_C$ into XhoI site of the NS2.2 (Gm^R; gentamicin resistance) targeting vector. The DNA sequence for P*sigF2*::*sigF2*-GSGS-3XFLAG$_C$ was generated by a series of nested PCR reactions. The P*sigF2* was taken as the 600 base pairs of sequence located upstream of the *sigF2* translation start codon (chromosomal sequence 1851929 to 1852528 bps). The *sigF2*-GSGS-3XFLAG$_C$ was generated by appending the coding sequence of *sigF2* (chromosomal sequence 1852529 to 1853311 bps) to the DNA sequence for the GSGS-3XFLAG epitope tag (GGCAGCGGCA GCGATTACAA AGATCACGAT GGCGATTACA AAGATCACGA TATCGATTAC AAAGATGATG ATGATAAA) which itself was appended to the DNA sequence for a stop codon (TAG).

vi. The KF-P-16 plasmid was constructed by insertion of P*sigF2*::*sigF2*-GSGS-3XFLAG$_C$ sequence from KF-P-08 into SalI site of the NS1 (Sp^R; spectinomycin resistance) targeting vector (pAM1303).

vii. The KF-P-75 plasmid was constructed by insertion of DNA homologous to sequence located upstream of the *rpoD6* coding sequence, nourseothricin resistance cassette (Nat^R; nourseothricin resistance), and DNA homologous to sequence located downstream of the

rpoD6 coding sequence into the KpnI site of the puc18 vector (ATCC 37253). The insert DNA sequence was generated by a series of nested PCR reactions: stitching the DNA sequence of chromosomal position 1612464 to 1613464 bps to the DNA sequence of the nourseothricin resistance cassette (Nat^R: AAGCAGGCTG AGCAGGTTTT AATTCTCATG TTTGACAGCT TATCATCGAA TTATAGGAAT AGAGCAAACA AGCAAAGGAA ATTTTGTCAA AATAATTTTA TTGACAACGT CTTATTAACG TTGATATAAT TTAAATTTTA TTTGACAAAA ATGGGCTCGT GTTGTACAAT AAATGTAGTG AGGTGGATGC AATGGCGATG ACGTTGTCCG ATATTAAAAG ATCGCTTGAT GGGAATTTAG GTAAAAGGCT GACGTTAAAA GCAAACGGTG GCCGGATCCA TATGACCACC CTGGATGATA CCGCCTACCG CTACCGCACC AGCGTTCCCG GTGATGCCGA AGCCATCGAA GCCCTGGATG GCAGCTTTAC CACCGATACC GTGTTTCGCG TGACCGCCAC GGGTGATGGC TTTACCCTGC GCGAAGTGCC CGTCGATCCC CCTCTGACCA AAGTGTTTCC CGATGATGAA AGTGATGATG AATCGGATGC TGGCGAAGAT GGCGATCCCG ATAGCCGCAC CTTTGTGGCC TACGGTGATG ATGGCGATCT GGCTGGCTTT GTGGTGGTGA GCTACAGCGG CTGGAATCGC CGCTTGACCG TGGAAGATAT TGAAGTGGCT CCCGAACACC GCGGTCACGG CGTTGGTCGC GCTCTGATGG GCCTGGCCAC CGAATTTGCT CGCGAACGCG GTGCTGGCCA CCTGTGGCTGG AAGTGACCAA CGTGAACGCTC CCGCTATCCA CGCCTATCGC CGCATGGGCT TCACCCTGTG TGGCCTGGAT ACCGCTCTGT ACGATGGCAC CGCCAGTGAT GGCGAACAGG CCCTGTACAT GAGCATGCCC TGCCCCTAAG GCCGGCCAGC CCGCCTAATG AGCGGGCTTT TTTTT) to the DNA sequence of chromosomal position 1614396 to 1615396 bps.

viii. The KF-P-76 plasmid was constructed by insertion of DNA homologous to sequence located upstream of the *rpoD5* coding sequence, nourseothricin resistance cassette (Nat^R; nourseothricin resistance), and DNA homologous to sequence located downstream of the *rpoD5* coding sequence into the KpnI site of the puc18 vector (ATCC 37253). The insert DNA sequence was generated by a series of nested PCR reactions: stitching the DNA sequence of chromosomal position 1915620 to 1916619 bps to the DNA sequence of the nourseothricin resistance cassette to the DNA sequence of chromosomal position 1917816 to 1918816 bps.

ix. The KF-P-78 plasmid was constructed by insertion of DNA homologous to sequence located upstream of the *sigF2* coding sequence, nourseothricin resistance cassette (Nat^R; nourseothricin resistance), and DNA homologous to sequence located downstream of the *sigF2* coding sequence into the KpnI site of the puc18 vector (ATCC 37253). The insert DNA sequence was generated by a series of nested PCR reactions: stitching the DNA sequence of chromosomal position 1851529 to 1852528 bps to the DNA sequence of the nourseothricin resistance cassette to the DNA sequence of chromosomal position 1853311 to 1854311 bps.

x. The KF-P-79 plasmid was constructed by insertion of DNA homologous to sequence located upstream of the *rpoD2* coding sequence, the nourseothricin resistance cassette (Nat^R; nourseothricin resistance), and DNA homologous to sequence located downstream of the *rpoD2* coding sequence into the KpnI site of the puc18 vector (ATCC 37253). The insert DNA sequence was generated by a series of nested PCR reactions: stitching the DNA sequence of chromosomal position 1815600 to 1816599 bps to the DNA sequence of the nourseothricin resistance cassette to the DNA sequence of chromosomal position 1817562 to 1818562 bps.

xi. The KF-P-80 plasmid was constructed by insertion of DNA homologous to sequence located upstream of the *rpoD2* coding sequence, the nourseothricin resistance cassette (Nat^R; nourseothricin resistance), DNA homologous to sequence located upstream of the *synpcc7942_0456* coding sequence, and coding sequence of *rpoD2* into the KpnI site of the puc18 vector (ATCC 37253). The insert DNA sequence was generated by a series of nested PCR reactions: stitching the DNA sequence of chromosomal position 1817770 to 1818427 bps to the DNA sequence of the nourseothricin resistance cassette to the DNA sequence of chromosomal position 444209 to 445208 bps to the DNA sequence of chromosomal position 1816600 to 1817562 bps.

Cyanobacterial strain construction

Strains were constructed using standard procedures for genomic integration by homologous recombination (Clerico et al., 2007). All strains were analyzed by colony PCR to verify target integration into the genome. Strain AMC408 was a gift from Dr. Susan Golden (University of California, San Diego).

Table 1. Cyanobacterial strains used in this study

Strain description	Strain genotype	Strain construction
FLAG-tagged RpoD6	NS2::P*purF::luxAB* (NS2, Cm^R targeting vector) NS1::P*psbA1::luxCDE* (NS1 Sp^R targeting vector), *rpoD6::Km*^{R}, NS2.2::P*rpoD6::rpoD6-GSGS-3XFLAGc* (NS2.2 Gm^R targeting vector)	AMC408 transformed with pAG(plasmid for replacing *rpoD6* coding locus with Km^R; gift of Andrian Gutu) and KF-P-06
FLAG-tagged RpoD5	NS2::P*purF::luxAB* (NS2 Cm^R targeting vector) NS1::P*psbA1::luxCDE* (NS1 Sp^R targeting vector), *rpoD5::Km*^{R}, NS2.2::P*rpoD5::rpoD5-GSGS-3XFLAGc* (NS2.2 Gm^R targeting vector)	AMC408 transformed with pAG(plasmid for replacing *rpoD5 coding* locus with Km^R; gift of Andrian Gutu) and KF-P-05
FLAG-tagged SigF2	NS2::P*purF::luxAB* (NS2 Cm^R targeting vector) NS1::P*psbA1::luxCDE* (NS1 Sp^R targeting vector), *sigF2::Km*^{R}, NS2.2::P*sigF2::sigF2-GSGS-3XFLAGc* (NS2.2 Gm^R targeting vector)	AMC408 transformed with pAG(plasmid for replacing *sigF2* coding locus with Km^R; gift of Andrian Gutu) and KF-P-08
OX-D53E	*kaiBC::Cm*^{R}, *rpaA::Km*^{R}, NS2.2::P*trc::rpaA(D53E)* (NS2.2 Gm^R targeting vector)	Described in Markson et al. 2013
OX-D53E lacking *rpoD2*	*kaiBC::Cm*^{R}, *rpaA::Km*^{R}, NS2.2::P*trc::rpaA(D53E)* (NS2.2 Gm^R targeting vector), *rpoD2*Δ	OX-D53E transformed with KF-P-79
OX-D53E with P*sypncc7942_0456* replacing P*rpoD2*	*kaiBC::Cm*^{R}, *rpaA::Km*^{R}, NS2.2::P*trc::rpaA(D53E)* (NS2.2 Gm^R targeting vector), P*sypncc7942_0456::rpoD2*	OX-D53E transformed with KF-P-80
OX-D53E lacking *rpoD6*	*kaiBC::Cm*^{R}, *rpaA::Km*^{R}, NS2.2::P*trc::rpaA(D53E)* (NS2.2 Gm^R targeting vector), *rpoD6::Nat*^{R}	OX-D53E transformed with KF-P-75
OX-D53E lacking *rpoD5*	*kaiBC::Cm*^{R}, *rpaA::Km*^{R}, *NS2.2::Ptrc::rpaA(D53E) (NS2.2 Gm*^{R} *targeting vector), rpoD5::NatR*	OX-D53E, transformed with KF-P-76
Wild-type lacking *sigF2*	*sigF2::Nat*^{R}	ATCC PCC 7942, transformed with KF-P-78
OX-D53E lacking rpoD6 with FLAG-tagged RpoD6	*kaiBC::Cm*^{R}, *rpaA::Km*^{R}, NS2.2::P*trc::rpaA(D53E)* (NS2.2 Gm^R targeting vector), *rpoD6::Nat*^{R}, NS1::P*rpoD6::rpoD6-GSGS-3XFLAGc* (NS1 Sp^R targeting vector)	OX-D53E transformed with KF-P-75 and KF-P-14
OX-D53E lacking *rpoD5* with FLAG-tagged RpoD5	*kaiBC::Cm*^{R}, *rpaA::Km*^{R}, *NS2.2::Ptrc::rpaA(D53E) (NS2.2 Gm*^{R} *targeting vector), rpoD5::Nat*^{R}, NS1::P*rpoD5::rpoD5-GSGS-3XFLAGc* (NS1 Sp^R targeting vector)	OX-D53E transformed with KF-P-76 and KF-P-13
OX-D53E lacking sigF2 with FLAG-tagged SigF2	*kaiBC::Cm*^{R}, *rpaA::Km*^{R}, *NS2.2::Ptrc::rpaA(D53E) (NS2.2 Gm*^{R} *targeting vector), sigF2::Nat*^{R}, NS1::P*sigF2::sigF2-GSGS-3XFLAGc* (NS1 Sp^R targeting vector)	OX-D53E transformed with KF-P-78 and KF-P-16

Cyanobacterial growth conditions

Cultures were grown in tissue culture flasks (Fischer Scientific) illuminated with 100 mE m^{-2} s^{-1} (mmoles photons m^{-2} s^{-1}) of cool fluorescent light and bubbled continuously with 1% CO_2 in air. Cell density was maintained near OD_{750nm} near 0.3 by measuring OD_{750nm} every 2 h and making necessary dilutions with fresh BG-11 medium supplemented with 10 mM HEPES-KOH pH 8.0 to maintain pH. Cultures were exposed to two 12h light–12h dark cycles (light: 100 mE m^{-2} s^{-1} of cool fluorescent light) at 30°C for entrainment before release into constant light (100 mE m^{-2} s^{-1} of cool fluorescent light) at 30°C. For phosphomimetic RpaA mutant overexpression experiments, cultures were grown initially in absence of IPTG, treated with two 12h light-12h dark cycles, and released into constant light (100 mE m^{-2} s^{-1}) concomitant with addition of IPTG to a final concentration of 100 μM.

Western blot analysis

Cells from 15 ml of culture were harvested by vacuum filtration onto cellulose acetate filters (Whatman). Filters were flash-frozen in liquid nitrogen and stored at -80°C until lysis. To prepare lysates, cells were eluted from the filters using 300 μl ice-cold lysis buffer (7.5 M urea, 20 mM HEPES pH 8.0, 1 mM DTT, and 1 Roche Complete protease inhibitor tablet per 50 ml, with 1 mM EDTA). Resuspensions were transferred to 500 μl screw-cap tubes containing 0.1 mm glass beads (Fischer Scientific). Cells were lysed by bead-beating resuspensions at 4 C for six cycles of 30 sec each separated by at least 30 sec of cooling on ice. To clarify cellular debris, the lysates were centrifuged 10 min at 14,000 x *g* at 4°C; after which the supernatants were transferred to new microcentrifuge tubes. The total protein content of each sample was measured by Bradford assay (Bio-Rad) using bovine serum albumin (BSA, Bio-Rad) diluted over 10-fold

range into lysis buffer to generate a standard curve of protein concentration versus OD_{595nm} value measured by Bradford assay. For each western blot, an equal mass quantity of each lysate was loaded to respective lanes of a SDS-PAGE gel (4-20% Novek Tris-Glycine, Invitrogen). SDS-PAGE gels were run at 150 V for 1.5 h at 4°C, after which gels were transferred to nitrocellulose membrane using semi-dry apparatus run at constant Volt/Amp setting for 1 h at 25°C. Blots were then incubated with 5% milk (Skim milk powder, VWR) in TBST for 1 h at 4 C to block non-specific binding of proteins to primary antibody, and probed with primary antibody (anti-FLAG M2, Sigma-Aldrich, 1:1000 dilution; anti-RpaA, Gutu and O'Shea 2013, 1:1000 dilution) diluted in 5% TBST overnight at 4°C. To disturb non-specific binding interactions and to remove unbound primary antibody, blots were washed with TBST for 10 min three consecutive times. Secondary antibody (Goat Anti-Mouse IgG-HRP Conjugate, Bio-Rad #1721011 at 1:12500 dilution; Goat Anti-Rabbit IgG, Peroxidase Conjugated, Pierce Biotechnology #32460 at 1:1000 dilution) diluted in 5% TBST was incubated with respective blots for 1 h at 25°C. To disturb non-specific binding interactions and remove unbound secondary antibody blots were washed with TBST for 10 min three consecutive times. Bands were visualized using Super Signal West Femto Maximum Sensitivity Substrate kit (Fischer Scientific) and AlphaImager EP software (Alpha Innotech). For measuring RpaA phosphorylation we implemented modifications to the above western blotting procedure as previously described for Phos-tag (Gutu and O'Shea, 2013).

Chromatin immunoprecipitation

For each chromatin immunoprecipitation (ChIP) reaction, approximately 18 $OD_{750\ nm}$ units of culture were crosslinked for 15 min with 1% formaldehyde followed by quenching for 5 min with 125 mM glycine. For the chromatin immunoprecipitation of epitope-tagged RNA

polymerase (gift of A. Puszynska), cells were treated with rifampicin for 20 min at 30°C prior to crosslinking with 1% formaldehyde and quenching with 125 mM glycine. Cells were collected by centrifugation for 10 min at 6000 x *g* at 4°C and then washed twice with 30 ml of ice-cold phosphate-buffered saline (PBS), centrifuging for 10 min at 3000 x *g* at 4 C after each wash. Samples were then resuspended in 1 ml ice-cold PBS and pelleted in a microcentrifuge tube for 3 min at 3000 x *g* at 4°C. The supernatant was discarded and the pellet was flash frozen in liquid nitrogen and stored at 80 C. Samples were thawed on ice and resuspended in 300 µl of ice-cold lysis buffer (50 mM HEPES pH 7.5, 140 mM NaCl, 1 mM EDTA, 1% Triton X-100, 0.1% sodium deoxycholate, and 1x Roche Complete EDTA-free Protease Inhibitor Cocktail). Cells were lysed by bead beating at 4°C in 2 ml screw-top tubes with 0.1 mm glass beads for 10 cycles of 30 s each separated by at least 30 s of cooling on ice. Lysate was separated from the beads by piercing the bottom of each tube with a small-diameter needle, placing the tube into a clean 1.5 ml microcentrifuge tube, and centrifuging for several minutes at 1000 x *g* at 4°C to transfer the lysate to the 1.5-ml tube. Chromatin was then sheared to a length of 250-400 bp by sonication at 4°C in Covaris S220 sonicator with settings: peak incident power 175, duty factor 10, cycles per burst 200, time 160 s. Cell debris was removed by centrifuging twice at 14,000 x *g* for 15 min each at 4 C. Protein concentration in the lysates was determined by BCA assay using BSA as a standard. For a given ChIP time-course, equal mass quantities (typically 1 mg) of lysate from each time point were prepared in 500 ul of lysis buffer each. For anti-FLAG ChIP, 40 ul (bed volume) of anti-FLAG magnetic beads (Sigma) equilibrated in lysis buffer were added to each tube. Samples were incubated overnight in the dark at 4°C with continuous rotation. Beads were isolated by placement on magnetic stand for 1 min. Beads were then washed twice with 1 ml lysis buffer, once with 1 ml of buffer B (50 mM HEPES pH 7.5, 500 mM NaCl, 1 mM EDTA,

1% Triton X-100, 0.1% sodium deoxycholate), once with 1 ml of wash buffer (10 mM TrisCl pH 8.0, 250 mM LiCl, 1 mM EDTA, 0.5% NP-40, 0.1% sodium deoxycholate) and finally with 1 ml of TE pH 7.5 (10 mM TrisCl pH 7.5, 1 mM EDTA); each wash was conducted for 5 min at room temperature on a tube rotator followed by isolation of beads by centrifugation for 1 min at 1000 x *g* at 25°C. Protein-DNA complexes were then eluted with 250 µl elution buffer (50 mM TrisCl pH 8.0, 10 mM EDTA, 1% SDS) for 1 hr at 65°C. For both the eluate and a matched sample of lysate not subjected to immunoprecipitation, crosslinks were reversed for 6-18 hr at 65°C. Next, 250 µl of TE was added to each sample to dilute the SDS, followed by addition of 100 µg of proteinase K and 80 µg of glycogen. Samples were incubated for 2 hr at 37°C to digest proteins. Samples were then supplemented with 55 µl of 4 M LiCl and extracted with 1 ml of phenol/chloroform/isoamyl alcohol followed by extraction with 1 ml chloroform. DNA in the aqueous phase was precipitated with 0.3 M NaOAc pH 5.2 and 1 ml ethanol at for 1 h at -20°C. Precipitated DNA was pelleted by centrifugation 14000 x *g* at 4°C for 30 min. Pellets were air-dried and then resuspended in 50 µl of TE containing 20 ng/ml of DNase-free RNase (Fermentas) and incubated for 1 hr at 37°C to digest RNA. Samples were then supplemented with 150 µl of TE and 22.2 µl of 3 M sodium acetate pH 5.2, extracted with phenol/chloroform/isoamyl alcohol, and precipitated with 0.3 M NaOAc and ethanol for 1 h at -20°C. Precipitated DNA was pelleted by centrifugation 14000 x *g* at 4°C for 30 min. Pellets were air-dried and then resuspended in 50 µl of TE. DNA concentration in ChIP samples was estimated by PicoGreen assay (Invitrogen). Typical immunoprecipitation efficiencies (fraction of flag-tagged sigma factor depleted from the lysate) were greater than 50%.

ChIP-Seq library preparation and sequencing

Libraries for Illumina sequencing of ChIP DNA were prepared following a protocol developed by Ethan Ford (http://ethanomics.files.wordpress.com/2012/09/chip_truseq.pdf), with modifications. Specifically, 0.15-3 ng of ChIP DNA was used for each sample. DNA ends were blunted by treatment with 1.4 units of T4 DNA polymerase (NEB), 0.45 units of Klenow fragment (NEB), 4.5 units of T4 polynucleotide kinase (NEB), and 0.4 mM dNTPs (NEB) in 1x T4 DNA ligase buffer (NEB) in a total of 50 µl volume for 30 min at 20°C. DNA was purified using 50 µl of AMPure XP beads (Beckman) and 50 µl of a solution containing 20% PEG8000 (Sigma) and 1.25 M NaCl. DNA was eluted in 16.5 µl of TE/10 (10 mM TrisCl pH 8.0, 0.1 mM EDTA). DNA was then A-tailed at the 3' ends by treating the eluate with 2.5 units of Klenow fragment lacking 3' to 5' exonuclease activity (NEB) and 0.2 mM dATP (GE Healthcare) in 1x NEB Buffer 2 (NEB) in a total volume of 20 µl for 30 min at 37°C. TruSeq adapters (Eurofins MWG Operon) were ligated onto the A-tailed DNA by addition of 25 µl of 2X Quick Ligase Buffer (NEB), 0.5 µl of 250 nM TruSeq adaptor, 3 µl of nuclease-free H_2O, and 1.5 µl of Quick Ligase (NEB) followed by incubation for 20 min at 21°C. The ligation reaction was stopped by addition of 5 µl of 0.5 M EDTA pH 8.0 (Ambion). Next, DNA was purified using 55 µl of AMPure XP beads without additional PEG or salt. DNA was eluted in 15.5 µl of TE/10. The Y-shaped adapters were then linearized with 5 cycles of PCR (initial denaturation of 30 s at 98 C followed by 5 cycles of [10 sec at 98°C, 30 sec at 60°C, 30 sec at 72°C] followed by 5 min at 72°C) using Phusion polymerase (Life Technologies) and 1 µl of TruSeq primers (25 µM) in a total volume of 31 µL. Linearized DNA was purified using 30 µl of AMPure XP beads without additional PEG or salt. DNA was eluted in 30 µl of TE/10. Fragments between 300 and 500 base pairs in length were size-selected using agarose gel purification and the QIAquick gel extraction

kit (QIAGEN). Purified DNA was further amplified with 13-14 cycles of PCR, as described above, in a total volume of 62.5 µl. Following PCR, DNA was purified using 51 µl of AMPure XP beads without additional PEG or salt. DNA was eluted in 12 µl of TE/10. Average fragment sizes for libraries were assessed using a DNA High Sensitivity chip on Agilent 2200 Tapestation. Samples were sequenced at the Harvard FAS Center for Systems Biology. Reads were aligned to the *S. elongatus* genome (chromosome: NC_007604.1; plasmids: NC_004073.2 and NC_004990.1) using Bowtie (Langmead et al., 2009) counting only those aligned uniquely to one location with up to three mismatches.

ChIP-Seq data analysis

Data were analyzed using a modified form of the PeakSeq algorithm (Rozowsky et al., 2009) that narrows the regions identified as peaks by requiring that each 50-bp window within a putative peak be enriched ($p < 0.05$) relative to mock ChIP (as described by Markson et al. 2013). The fold enrichment for each peak was calculated by finding the maximum ChIP-to-mock ratio within 50 bp of the location of the peak maximum in the raw ChIP-Seq signal.

Identification of reproducible circadian genes

In order to focus our analysis on genes that show reproducible circadian oscillations, we restricted analysis a subset (n=336) of the 856 high-confidence circadian coding genes previously annotated (Markson et al., 2013) that exhibit greater than 1.75 ratio peak to trough expression in wild-type cells grown in constant light conditions and have a transcription start site located within 250 bp upstream of their start codons; transcription start sites were annotated genome-wide (this work) by performing circadian timecourse ChIP-seq on cells with functional,

epitope-tagged RNA polymerase (gift of A. Puszynska) treated with rifampicin (Sigma-Aldrich) to lock RNA polymerase at initiation sites genome-wide.

Isolation of total RNA

Cells from 50 ml of culture were harvested by vacuum filtration onto nitrocellulose filters (Whatman). Filters were flash-frozen in liquid nitrogen and stored at -80°C until lysis. To prepare lysates, cells were eluted from the filters using 12 ml of ice-cold AE buffer (50 mM NaOAc pH 5.2, 0.5 M EDTA, DEPC treated water). Cell suspensions were transferred to SS34 tubes and lysed by addition of 800 µl of 25% SDS and 12 mL unbuffered acid phenol (pH 4.3). Cells were lysed for 10 min while being incubated in 65°C water bath and intermittently vortexed. Lysates were incubated 5 min on ice. Cell debris were pelleted by centrifugation at 12000 rpm at 4°C for 30 min. Supernatants were transferred to phase lock heavy tubes with 12 ml chloroform and centrifuged for 10 min at 3000 rpm. Nucleic acids in supernatants were precipitated for 1 h at -20°C in presence of 1 mL 3 M NaOAc pH 5.2 and 10 mL isopropanol. Precipitated nucleic acids were pelleted by centrifugation at 12000 rpm at 4°C for 30 min. Cell pellets were washed with 5 mL 70% EtOH and pelleted by centrifugation at 12000 rpm at 4°C for 10 min. The supernatants were discarded and pellets were air dried at 25°C for 1 h. Pellets were resuspended in 500 µl of TE containing 25 µl of Promega RQ1 RNAse free DNAse (1000 Units/ml) and incubated for 1 h at 37°C to digest DNA. Samples were extracted with equal volume phenol/chloroform/isoamyl alcohol and precipitated at -20°C in presence of 0.3 M NaOAc pH 5.2 and 1 mL ethanol. Precipitated nucleic acids were pelleted by centrifugation at 12000 rpm at 4°C for 30 min, air-dried at 25°C for 1 h, and resuspended in 50 µl of nuclease free water. The quality of the isolated total RNA was estimated by the ratio of absorbance at 260 nm

to 280 nm. The presence of contaminating DNA was checked by setting up PCR reactions with a 1000-fold range of resuspended cell pellets and assessing by gel electrophoresis. Samples containing isolated and high-quality total RNA free of contaminating DNA were flash frozen and stored at -80°C.

qPCR for gene expression

RT-qPCR was performed on isolated total RNA as described previously (Vijayan and O'Shea, 2013).

Table 2. Primers used for RT-qPCR in this study

Target	RT-qPCR Primers		Reference
sypncc7942_0905	F:	TATATCTACTAAGTGGGACTGTG	This work
	R:	CCTAAAGTGAAGTCACTATTAGT	
synpcc7942_0004	F:	ACTTGGTCAACACGGTTG	This work
	R:	ATCGTCAGGCTAAAGGC	
sypcc7942_1760	F:	CAGATCTGGATCGAGCAA	This work
	R:	GGCTCCTTAACCTTGACAA	
sypncc7942_0834	F:	CAATGTCACCCTCATTAATGG	This work
	R:	AGCAAGTAATCGGCTTCAA	
sypncc7942_1746	F:	TTCTGCCATTAAATTGCGTAG	This work
	R:	GGAATACATCCAAATGAAC	
sypncc7942_1849	F:	CGAGGACTAGAGCTTCTC	This work
	R:	CGAATCGTCCGACTTTG	
sypncc7942_1557	F:	AGGAAACTCTTGCCATC	This work
	R:	TGAGCCAAATCCGCAAA	
sypncc7942_1784	F:	TGTTCAGCTCAATCTAGGG	This work
	R:	GTATATAGGGCACTGCAAAG	
sypncc7942_0599	F:	CAGACCAACTGATTCGAGCG	Vijayan and O'Shea 2013
	R:	GGAGGCCAGGAGCAGTC	

RNA-seq library preparation and sequencing

Ribosomal RNA was depleted from 500 ng of isolated total RNA using the Ribo-Zero rRNA removal kit (Illumina) according to manufacturer's instructions. Strand-specific RNA-sequencing libraries were prepared from 100 ng of rRNA-depleted RNA using the TruSeq Stranded mRNA Sample Prep Kit (Illumina). Samples were multiplexed and sequenced on an Illumina HiSeq machine by the core facility at the Harvard FAS Center for Systems Biology. Reads were aligned to the *S. elongatus* genome (chromosome: NC_007604.1; plasmids: NC_004073.2 and NC_004990.1) using Bowtie (Langmead et al., 2009) counting only those aligned uniquely to one location with up to three mismatches. To quantify gene expression, we summed the number of sequencing reads with 5' end between start and stop positions of

annotated mRNA, tRNA, rRNA, and high-confidence noncoding RNA (Vijayan et al., 2011). We performed median normalization (described in Anders and Huber, 2010; Markson et al., 2013) to normalize gene expression values between samples.

References

Dunlap JC. (1999). Molecular bases for circadian clocks. Cell. *96* (2): 271-90.

Dunlap JC, Loros JJ, De Coursey PJ, eds 2004. Chronobiology: Biological Timekeeping. Sunderland, MA: Sinauer. 406 pp.

Bell-Pedersen, D., Cassone, V.M., Earnest, D.J., Golden, S.S., Hardin, P.E., Thomas, T.L., and Zoran, M.J. (2005). Circadian rhythms from multiple oscillators: lessons from diverse organisms. Nat. Rev. Genet. *6*, 544–556.

Liu, Y., Tsinoremas, N., Johnson, C., Lebdeva, N., Golden, S., Ishiura, M., and Kondo, T. (1995). Circadian orchestration of gene expression in cyanobacteria. Genes Dev. *9*, 1469–1478.

Golden, S., Ishiura, M., Johnson, C.H., and Kondo, T. (1997). Cyanobacterial circadian rhythms. Annu. Rev. Plant Physiol. Plant Mol. Biol. *48*, 327–354.

Ito, H., Mutsuda, M., Murayama, Y., Tomita, J., Hosokawa, N., Terauchi, K., Sugita, C., Sugita, M., Kondo, T., and Iwasaki, H. (2009). Cyanobacterial daily life with Kai-based circadian and diurnal genome-wide transcriptional control in Synechococcus elongatus. Proc. Natl. Acad. Sci. USA *106*, 14168–14173.

Vijayan, V., Zuzow, R., and O'Shea, E.K. (2009). Oscillations in supercoiling drive circadian gene expression in cyanobacteria. Proc. Natl. Acad. Sci. USA *106*, 22564–22568.

Ouyang, Y., Andersson, C.R., Kondo, T., Golden, S.S., and Johnson, C.H. (1998). Resonating circadian clocks enhance fitness in cyanobacteria. Proc. Natl. Acad. Sci. USA *95*, 8660–8664.

Woelfle MA, Ouyang Y, Phanvijhitsiri K, Johnson CH. (2004). The adaptive value of circadian clocks: an experimental assessment in cyanobacteria. Curr. Biol. *14*, 1481–1486.

Diamond S, Jun D, Rubin BE, Golden SS. *(*2015). The circadian oscillator in Synechococcus elongatus controls metabolite partitioning during diurnal growth. Proc Natl Acad Sci USA *112,* E1916–E1925.

Nishiwaki T, Satomi Y, Kitayama Y, Terauchi K, Kiyohara R, Takao T, Kondo T. (2007). A sequential program of dual phosphorylation of KaiC as a basis for circadian rhythm in cyanobacteria. EMBO J. *26*, 4029–37.

Rust MJ, Markson JS, Lane WS, Fisher DS, O'Shea EK. (2007). Ordered phosphorylation governs oscillation of a three-protein circadian clock. Science *318*, 809–812.

Takai N, Nakajima M, Oyama T, Kito R, Sugita C, Sugita M, Kondo T, Iwasaki, H. 2006. A KaiC associating SasA–RpaA two-component regulatory system as a major circadian timing mediator in cyanobacteria. Proc. Natl. Acad. Sci. USA *103*, 12109–14.

Gutu A, O'Shea EK. (2013). Two antagonistic clock-regulated histidine kinases time the activation of circadian gene expression. Mol. Cell *50*, 288–94.

Markson JS, Piechura JR, Puszynska AM, O'Shea EK. (2013). Circadian control of global gene expression by the cyanobacterial master regulator RpaA. Cell *155*, 1396-1408.

Feklistov A, Sharon BD, Darst SA & Gross CA. (2014). Bacterial sigma factors: a 713 historical, structural, and genomic perspective. Annu. Rev. Microbiol. *68*, 357–376

Imamura S , Asayama M. (2009). Sigma factors for cyanobacterial transcription. Gene Regul. Syst. Bio. *3*, 65–87.

Gross C, Chan C, Dombroski A, Gruber T, Sharp M, et al.. (1998) The functional and regulatory roles of sigma factors in transcription. In: Cold Spring Harbor symposia on quantitative biology. Cold Spring Harbor Laboratory Press, *63*, 141–156.

Ishihama A. (2000). Functional modulation of Escherichia coli RNA polymerase. Annual Reviews in Microbiology *54*, 499–518.

Gruber TM and Gross CA. (2003). Multiple sigma subunits and the partitioning of bacterial transcription space. Annual Review of Microbiology *57*, 441–466.

Nair U, Ditty JL, Min H, Golden SS. (2002). Roles for sigma factors in global circadian regulation of the cyanobacterial genome. J. Bacteriol. *184*, 3530–38.

Espinosa J, Boyd J, Cantos R, Salinas P, Golden S, Contreras A. (2015). Cross-talk and regulatory interactions between the essential response regulator RpaB and cyanobacterial circadian clock output. Proc Natl Acad Sci U S A *112*, 2198–2203.

Anders, S. & Huber, W. (2010). Differential expression analysis for sequence count data. Genome Biol. *11*, R106.

Clerico EM, Ditty JL, Golden SS. (2007). Specialized techniques for site-directed mutagenesis in cyanobacteria. Methods Mol. Biol. *362*, 155–171.

Supplementary Table 1. Location of transcription start sites for high-confidence circadian genes determined by analysis of time-course ChIP-seq datasets for RNA polymerase locked at initiation sites genome-wide by rifampicin treatment

Supplementary Table 1 (Continued).

Transcript information						Genomic location (bp) of maximum ChIP-seq signal from RNA polymerase locked at initiation site by rifampicin							Upstream distance (bp) of 5'TSS to translation start
JGI ID	Synpcc_7942 number	Strand ('+' direct; '-' complement), Genome, Translation start (bp)			Ratio of peak to trough expression	T=24 h	T=28 h	T= 32 h	T= 36h	T= 40h	T= 44 h	Mean	
637798409	'Synpcc7942_0004'	'+'	Chromosome	4596	3.3	4543	4540	4542	4542	4542	4540	4542	54
637798419	'Synpcc7942_0014'	'-'	Chromosome	13411	1.8	13372	13420	13423	13419	13419	13365	13403	-8
637798424	'Synpcc7942_0019'	'+'	Chromosome	18615	3.2	18341	18473	18473	18471	18471	18316	18424	191
637798425	'Synpcc7942_0020'	'+'	Chromosome	20490	2.8	20541	20340	20367	20309	20309	20339	20368	122
637798427	'Synpcc7942_0022'	'-'	Chromosome	23049	2.0	23025	23350	23350	23350	23350	23350	23296	247
637798428	'Synpcc7942_0023'	'-'	Chromosome	24121	1.8	24161	24152	24159	24154	24154	24155	24156	35
637798431	'Synpcc7942_0026'	'-'	Chromosome	28059	1.8	28130	28162	28164	28163	28163	28159	28157	98
637798438	'Synpcc7942_0033'	'-'	Chromosome	33506	4.8	33807	33807	33807	33807	33807	33457	33749	243
637798444	'Synpcc7942_0039'	'+'	Chromosome	37130	10.6	37094	37098	37098	37096	37096	37096	37096	34
637798445	'Synpcc7942_0040'	'+'	Chromosome	38630	6.7	38601	38603	38603	38604	38604	38604	38603	27
637798475	'Synpcc7942_0069'	'+'	Chromosome	69079	5.2	68915	68919	68918	68919	68919	68917	68918	161
637798492	'Synpcc7942_0086'	'-'	Chromosome	84955	2.9	85036	85122	85120	85119	85119	85110	85104	149
637798496	'Synpcc7942_0090'	'+'	Chromosome	88735	1.9	88653	88650	88646	88647	88647	88647	88648	87
637798498	'Synpcc7942_0092'	'-'	Chromosome	90930	2.3	90886	90895	90881	90950	90950	90951	90919	-11
637798502	'Synpcc7942_0096'	'-'	Chromosome	94285	2.8	94316	94316	94315	94316	94316	94315	94316	31
637798506	'Synpcc7942_0100'	'-'	Chromosome	101082	4.4	101136	101136	101137	101139	101139	101138	101138	56
637798507	'Synpcc7942_0101'	'+'	Chromosome	101259	1.8	101136	101136	101137	101139	101139	101138	101138	121
637798509	'Synpcc7942_0103'	'-'	Chromosome	103645	3.3	103598	103946	103946	103944	103944	103946	103887	242
637798554	'Synpcc7942_0148'	'+'	Chromosome	148646	2.6	148613	148615	148620	148619	148619	148564	148608	38
637798567	'Synpcc7942_0161'	'+'	Chromosome	162764	2.3	162762	162760	162762	162763	162763	162762	162762	2
637798579	'Synpcc7942_0173'	'-'	Chromosome	173071	2.1	173081	173093	173090	173088	173088	173086	173088	17
637798611	'Synpcc7942_0205'	'+'	Chromosome	206198	1.9	206141	206141	206143	206142	206142	206142	206142	56
637798621	'Synpcc7942_0215'	'-'	Chromosome	217813	2.6	217839	217839	217839	217839	217839	217839	217839	26
637798642	'Synpcc7942_0236'	'+'	Chromosome	232018	1.9	231963	231967	231964	231941	231941	231952	231955	63
637798650	'Synpcc7942_0244'	'-'	Chromosome	241156	9.2	241388	241386	241383	241385	241385	241383	241385	229
637798651	'Synpcc7942_0245'	'-'	Chromosome	242229	19.7	242257	242259	242260	242262	242262	242275	242263	34
637798658	'Synpcc7942_0252'	'-'	Chromosome	248136	2.1	248261	248256	248252	248252	248252	248252	248254	118
637798662	'Synpcc7942_0256'	'+'	Chromosome	252873	2.1	252886	252839	252873	252873	252873	252875	252870	3
637798684	'Synpcc7942_0278'	'+'	Chromosome	273657	35.0	273560	273589	273561	273565	273565	273555	273566	91
637798685	'Synpcc7942_0279'	'+'	Chromosome	274154	6.0	273855	273936	273926	273939	273939	273880	273913	241
637798694	'Synpcc7942_0288'	'-'	Chromosome	283962	2.0	284090	284084	284085	284084	284084	284088	284086	124
637798697	'Synpcc7942_0291'	'+'	Chromosome	288312	2.0	288280	288287	288288	288288	288288	288246	288280	32
637798701	'Synpcc7942_0295'	'+'	Chromosome	291417	2.5	291349	291361	291356	291356	291356	291355	291356	61

Supplementary Table 1 (Continued)

637798710	'Synpcc7942_0304'	'+'	Chromosome	302833	36.6	302811	302811	302811	302810	302810	302811	302811	22
637798711	'Synpcc7942_0305'	'+'	Chromosome	303815	6.4	303776	303787	303789	303789	303789	303791	303787	28
637798718	'Synpcc7942_0312'	'-'	Chromosome	311708	4.3	311761	311754	311758	311757	311757	311738	311754	46
637798722	'Synpcc7942_0316'	'-'	Chromosome	314623	4.3	314724	314744	314769	314769	314769	314772	314758	135
637798737	'Synpcc7942_0331'	'+'	Chromosome	327926	2.0	327627	327965	327966	327966	327966	327969	327910	16
637798738	'Synpcc7942_0332'	'+'	Chromosome	328854	2.3	328792	328790	328789	328789	328789	328791	328790	64
637798742	'Synpcc7942_0336'	'+'	Chromosome	330878	2.0	330712	330929	330921	330929	330929	330872	330882	-4
637798744	'Synpcc7942_0338'	'+'	Chromosome	333517	2.5	333494	333479	333485	333481	333481	333486	333484	33
637798747	'Synpcc7942_0341'	'+'	Chromosome	335633	1.9	335600	335594	335593	335592	335592	335598	335595	38
637798755	'Synpcc7942_0349'	'-'	Chromosome	342443	1.8	342637	342625	342629	342629	342629	342629	342630	187
637798757	'Synpcc7942_0351'	'+'	Chromosome	343699	2.0	343626	343617	343617	343619	343619	343617	343619	80
637798775	'Synpcc7942_0369'	'+'	Chromosome	362147	15.3	362117	362105	362124	362124	362124	362102	362116	31
637798776	'Synpcc7942_0370'	'+'	Chromosome	363763	4.1	363657	363671	363659	363658	363658	363660	363661	102
637798783	'Synpcc7942_0377'	'-'	Chromosome	372206	2.4	372407	372220	372253	372291	372291	372408	372312	106
637798784	'Synpcc7942_0378'	'+'	Chromosome	372532	2.2	372407	372233	372253	372291	372291	372408	372314	218
637798789	'Synpcc7942_0383'	'-'	Chromosome	376448	3.3	376517	376481	376561	376517	376517	376483	376513	65
637798794	'Synpcc7942_0388'	'-'	Chromosome	381991	2.7	381952	382024	381963	381964	381964	381964	381972	-19
637798797	'Synpcc7942_0391'	'-'	Chromosome	385125	4.2	385233	385233	385230	385233	385233	385268	385238	113
637798800	'Synpcc7942_0394'	'-'	Chromosome	388220	2.4	388320	388247	388248	388312	388312	388458	388316	96
637798807	'Synpcc7942_0401'	'-'	Chromosome	395731	1.8	395794	395886	395888	395793	395793	395879	395839	108
637798817	'Synpcc7942_0411'	'-'	Chromosome	402991	2.0	403027	403022	403019	403016	403016	403019	403020	29
637798827	'Synpcc7942_0421'	'-'	Chromosome	411946	1.9	411984	412031	412101	412072	412072	412104	412061	115
637798828	'Synpcc7942_0422'	'+'	Chromosome	412147	2.6	411984	412031	412101	412072	412072	412104	412061	86
637798829	'Synpcc7942_0423'	'-'	Chromosome	413614	2.8	413798	413812	413816	413815	413815	413818	413812	198
637798873	'Synpcc7942_0466'	'+'	Chromosome	451838	3.6	451889	451825	451809	451803	451803	451817	451824	14
637798876	'Synpcc7942_0469'	'-'	Chromosome	456664	2.4	456727	456739	456735	456736	456736	456735	456735	71
637798889	'Synpcc7942_0482'	'-'	Chromosome	468773	1.8	469074	468780	468784	468789	468789	468811	468838	65
637798890	'Synpcc7942_0483'	'-'	Chromosome	469219	1.9	469365	469300	469262	469269	469269	469363	469305	86
637798892	'Synpcc7942_0485'	'+'	Chromosome	470975	2.0	470929	470928	470928	470928	470928	470929	470928	47
637798897	'Synpcc7942_0490'	'+'	Chromosome	477395	2.8	477339	477377	477382	477377	477377	477336	477365	30
637798898	'Synpcc7942_0491'	'+'	Chromosome	479700	3.5	479636	479637	479650	479649	479649	479652	479646	54
637798905	'Synpcc7942_0498'	'+'	Chromosome	484585	2.3	484529	484526	484529	484528	484528	484530	484528	57
637798906	'Synpcc7942_0499'	'-'	Chromosome	488370	5.0	488557	488544	488476	488528	488528	488518	488525	155
637798912	'Synpcc7942_0505'	'-'	Chromosome	492867	1.9	492986	492986	492987	492988	492988	492986	492987	120
637798935	'Synpcc7942_0527'	'-'	Chromosome	512234	8.2	512271	512277	512277	512223	512223	512535	512301	67
637798937	'Synpcc7942_0529'	'+'	Chromosome	513543	2.9	513512	513513	513515	513512	513512	513512	513513	30
637798952	'Synpcc7942_0544'	'+'	Chromosome	526892	1.9	526793	526837	526842	526842	526842	526841	526833	59
637798964	'Synpcc7942_0556'	'-'	Chromosome	539219	12.9	539252	539250	539249	539251	539251	539256	539252	33

Supplementary Table 1 (Continued).

637798976	'Synpcc7942_0568'	'-'	Chromosome	550687	2.1	550712	550717	550711	550716	550716	550713	550714	27
637798977	'Synpcc7942_0569'	'-'	Chromosome	551653	2.3	551704	551704	551697	551699	551699	551702	551701	48
637798981	'Synpcc7942_0573'	'-'	Chromosome	555533	8.2	555649	555627	555636	555643	555643	555646	555641	108
637798989	'Synpcc7942_0581'	'-'	Chromosome	562981	19.3	562984	562984	562978	562932	562932	562932	562957	-24
637799006	'Synpcc7942_0595'	'-'	Chromosome	583398	2.2	583429	583425	583425	583430	583430	583430	583428	30
637799010	'Synpcc7942_0599'	'-'	Chromosome	588404	20.4	588434	588431	588430	588430	588430	588705	588477	73
637799011	'Synpcc7942_0600'	'-'	Chromosome	590060	2.6	590253	590259	590254	590254	590254	590255	590255	195
637799013	'Synpcc7942_0602'	'-'	Chromosome	591454	2.0	591571	591523	591522	591523	591523	591523	591531	77
637799020	'Synpcc7942_0609'	'+'	Chromosome	596382	1.9	596249	596326	596331	596330	596330	596325	596315	67
637799026	'Synpcc7942_0615'	'+'	Chromosome	605836	1.9	605727	605704	605704	605704	605704	605703	605708	128
637799028	'Synpcc7942_0617'	'-'	Chromosome	607688	2.3	607751	607750	607755	607757	607757	607757	607755	67
637799035	'Synpcc7942_0623'	'+'	Chromosome	613972	2.7	613950	613965	613950	613964	613964	613951	613957	15
637799042	'Synpcc7942_0630'	'+'	Chromosome	622432	2.3	622403	622409	622405	622407	622407	622406	622406	26
637799051	'Synpcc7942_0639'	'+'	Chromosome	630677	2.1	630567	630566	630566	630567	630567	630566	630567	110
637799056	'Synpcc7942_0644'	'+'	Chromosome	637075	4.5	637034	637034	637034	637035	637035	637033	637034	41
637799059	'Synpcc7942_0647'	'+'	Chromosome	641196	4.0	641163	641163	641163	641163	641163	641164	641163	33
637799061	'Synpcc7942_0649'	'-'	Chromosome	643966	1.9	644136	644128	644128	644128	644128	644131	644130	164
637799067	'Synpcc7942_0655'	'+'	Chromosome	650232	2.6	650159	650174	650174	650175	650175	650173	650172	60
637799080	'Synpcc7942_0668'	'-'	Chromosome	664446	3.9	664459	664456	664424	664420	664420	664419	664433	-13
637799082	'Synpcc7942_0670'	'+'	Chromosome	665121	1.9	665049	665049	665027	665039	665039	665002	665034	87
637799084	'Synpcc7942_0672'	'+'	Chromosome	666887	2.2	666799	666802	666789	666799	666799	666795	666797	90
637799085	'Synpcc7942_0673'	'+'	Chromosome	667849	2.6	667667	667597	667614	667633	667633	667611	667626	223
637799086	'Synpcc7942_0674'	'+'	Chromosome	669347	1.8	669205	669201	669203	669204	669204	669204	669204	143
637799089	'Synpcc7942_0677'	'-'	Chromosome	672462	2.5	672660	672662	672660	672661	672661	672662	672661	199
637799092	'Synpcc7942_0680'	'+'	Chromosome	674334	4.8	674297	674303	674299	674294	674294	674252	674290	44
637799099	'Synpcc7942_0687'	'+'	Chromosome	682128	1.8	681973	681966	681961	681966	681966	681967	681967	161
637799111	'Synpcc7942_0699'	'+'	Chromosome	691619	1.9	691609	691609	691624	691607	691607	691607	691611	8
637799115	'Synpcc7942_0703'	'+'	Chromosome	694072	5.2	693996	694043	694045	694044	694044	694041	694036	36
637799157	'Synpcc7942_0742'	'+'	Chromosome	735651	3.0	735654	735625	735625	735627	735627	735584	735624	27
637799171	'Synpcc7942_0756'	'+'	Chromosome	750406	3.4	750332	750337	750333	750333	750333	750346	750336	70
637799186	'Synpcc7942_0770'	'+'	Chromosome	762159	2.5	761863	761963	761943	761953	761953	761941	761936	223
637799196	'Synpcc7942_0780'	'-'	Chromosome	773958	2.0	774194	774168	774211	774189	774189	774209	774193	235
637799197	'Synpcc7942_0781'	'-'	Chromosome	776520	2.6	776551	776552	776552	776551	776551	776551	776551	31
637799205	'Synpcc7942_0789'	'-'	Chromosome	785167	2.7	785160	785464	785456	785455	785455	785457	785408	241
637799212	'Synpcc7942_0796'	'+'	Chromosome	791175	4.9	791067	791065	791071	791071	791071	791074	791070	105
637799213	'Synpcc7942_0797'	'+'	Chromosome	792010	12.3	791998	791998	791999	792000	792000	791999	791999	11
637799215	'Synpcc7942_0799'	'-'	Chromosome	794390	2.1	794412	794418	794416	794415	794415	794416	794415	25
637799225	'Synpcc7942_0808'	'-'	Chromosome	802980	2.0	803071	803073	803091	803093	803093	803080	803084	104

Supplementary Table 1 (Continued).

637799245	'Synpcc7942_0828'	'-'	Chromosome	823241	2.4	823333	823339	823340	823340	823340	823340	823339	98
637799246	'Synpcc7942_0829'	'+'	Chromosome	823506	2.8	823333	823339	823340	823340	823340	823340	823339	167
637799250	'Synpcc7942_0834'	'+'	Chromosome	828582	299.6	828516	828491	828491	828493	828493	828517	828500	82
637799252	'Synpcc7942_0836'	'-'	Chromosome	832182	3.0	832326	832248	832253	832256	832256	832253	832265	83
637799271	'Synpcc7942_0855'	'+'	Chromosome	853629	5.6	853550	853547	853548	853549	853549	853548	853549	80
637799274	'Synpcc7942_0858'	'+'	Chromosome	855893	3.5	855820	855828	855594	855797	855797	855803	855773	120
637799277	'Synpcc7942_0861'	'-'	Chromosome	865469	2.1	865610	865561	865554	865581	865581	865600	865581	112
637799278	'Synpcc7942_0862'	'+'	Chromosome	865596	3.2	865610	865561	865554	865581	865581	865600	865581	15
637799318	'Synpcc7942_0901'	'+'	Chromosome	909780	2.6	909678	909681	909681	909681	909681	909681	909681	99
637799322	'Synpcc7942_0905'	'+'	Chromosome	915588	7.2	915516	915518	915558	915547	915547	915513	915533	55
637799344	'Synpcc7942_0926'	'+'	Chromosome	932734	1.9	932584	932594	932594	932596	932596	932634	932600	134
637799353	'Synpcc7942_0935'	'-'	Chromosome	942838	Inf	943041	942987	942982	942986	942986	943134	943019	181
637799359	'Synpcc7942_0941'	'-'	Chromosome	947773	2.2	947813	947801	947798	947800	947800	947801	947802	29
637799364	'Synpcc7942_0946'	'+'	Chromosome	954141	2.0	954007	953963	953990	953998	953998	953999	953993	148
637799366	'Synpcc7942_0947'	'-'	Chromosome	956714	2.0	956784	956777	956776	956780	956780	956810	956785	71
637799367	'Synpcc7942_0948'	'-'	Chromosome	957546	4.6	957623	957536	957696	957706	957706	957705	957662	116
637799369	'Synpcc7942_0950'	'-'	Chromosome	959737	2.3	959895	959891	959891	959891	959891	959922	959897	160
637799386	'Synpcc7942_0967'	'+'	Chromosome	974099	2.0	974067	974059	974060	974059	974059	974059	974061	38
637799391	'Synpcc7942_0972'	'+'	Chromosome	979369	2.3	979172	979178	979177	979177	979177	979177	979176	193
637799408	'Synpcc7942_0989'	'-'	Chromosome	997822	5.1	997863	997862	997866	997867	997867	997865	997865	43
637799412	'Synpcc7942_0993'	'-'	Chromosome	1003145	1.9	1003169	1003180	1003174	1003176	1003176	1003175	1003175	30
637799430	'Synpcc7942_1010'	'-'	Chromosome	1022700	1.9	1022737	1022735	1022695	1022705	1022705	1022736	1022719	19
637799439	'Synpcc7942_1019'	'+'	Chromosome	1033300	1.8	1033284	1033257	1033267	1033266	1033266	1033271	1033269	31
637799462	'Synpcc7942_1040'	'+'	Chromosome	1054722	3.7	1054693	1054691	1054692	1054693	1054693	1054690	1054692	30
637799464	'Synpcc7942_1042'	'+'	Chromosome	1055645	3.5	1055570	1055609	1055612	1055614	1055614	1055505	1055587	58
637799479	'Synpcc7942_1057'	'+'	Chromosome	1067527	1.9	1067416	1067458	1067462	1067445	1067445	1067446	1067445	82
637799486	'Synpcc7942_1064'	'+'	Chromosome	1074007	3.2	1073923	1073933	1073934	1073950	1073950	1073955	1073941	66
637799492	'Synpcc7942_1068'	'+'	Chromosome	1079478	2.0	1079419	1079494	1079494	1079421	1079421	1079421	1079445	33
637799497	'Synpcc7942_1072'	'-'	Chromosome	1084322	2.3	1084351	1084351	1084351	1084351	1084351	1084352	1084351	29
637799499	'Synpcc7942_1074'	'-'	Chromosome	1085562	7.0	1085544	1085563	1085555	1085555	1085555	1085561	1085556	-6
637799519	'Synpcc7942_1093'	'-'	Chromosome	1111780	1.8	1111831	1111828	1111827	1111827	1111827	1111828	1111828	48
637799521	'Synpcc7942_1095'	'+'	Chromosome	1112853	5.7	1112831	1112832	1112833	1112834	1112834	1112836	1112833	20
637799522	'Synpcc7942_1096'	'-'	Chromosome	1114724	3.3	1114940	1114941	1114939	1114939	1114939	1114940	1114940	216
637799534	'Synpcc7942_1108'	'+'	Chromosome	1125373	4.6	1125135	1125144	1125141	1125137	1125137	1125136	1125138	235
637799555	'Synpcc7942_1129'	'+'	Chromosome	1148540	1.9	1148515	1148516	1148520	1148517	1148517	1148515	1148517	23
637799561	'Synpcc7942_1135'	'-'	Chromosome	1157931	2.1	1157955	1157994	1157996	1157995	1157995	1157993	1157988	57
637799576	'Synpcc7942_1150'	'-'	Chromosome	1175734	12.6	1175774	1175771	1175770	1175770	1175770	1175770	1175771	37
637799582	'Synpcc7942_1156'	'+'	Chromosome	1183497	17.1	1183294	1183300	1183302	1183302	1183302	1183303	1183301	196

Supplementary Table 1 (Continued).

637799585	'Synpcc7942_1159'	'-'	Chromosome	1193292	2.5	1193298	1193297	1193297	1193297	1193297	1193296	1193297	5
637799590	'Synpcc7942_1164'	'+'	Chromosome	1197417	35.1	1197226	1197231	1197233	1197229	1197229	1197229	1197230	187
637799618	'Synpcc7942_1191'	'+'	Chromosome	1220349	2.1	1220259	1220223	1220238	1220239	1220239	1220278	1220246	103
637799622	'Synpcc7942_1195'	'+'	Chromosome	1223721	2.4	1223614	1223685	1223689	1223689	1223689	1223495	1223644	77
637799625	'Synpcc7942_1198'	'-'	Chromosome	1227244	1.9	1227545	1227284	1227269	1227278	1227278	1227279	1227322	78
637799629	'Synpcc7942_1202'	'-'	Chromosome	1232980	1.9	1232958	1233006	1232999	1233002	1233002	1233001	1232995	15
637799637	'Synpcc7942_1209'	'-'	Chromosome	1235230	3.0	1235286	1235321	1235321	1235323	1235323	1235320	1235316	86
637799640	'Synpcc7942_1212'	'-'	Chromosome	1236090	4.3	1236177	1236198	1236186	1236196	1236196	1236211	1236194	104
637799643	'Synpcc7942_1214'	'+'	Chromosome	1237017	2.0	1237015	1237012	1237017	1237014	1237014	1237014	1237014	3
637799655	'Synpcc7942_1226'	'+'	Chromosome	1247104	2.0	1246982	1247008	1247006	1247008	1247008	1247003	1247003	101
637799656	'Synpcc7942_1227'	'-'	Chromosome	1249327	4.4	1249399	1249354	1249354	1249365	1249365	1249334	1249362	35
637799659	'Synpcc7942_1230'	'-'	Chromosome	1251846	2.4	1251903	1251870	1251861	1251868	1251868	1251874	1251874	28
637799661	'Synpcc7942_1232'	'-'	Chromosome	1253489	2.0	1253525	1253524	1253524	1253524	1253524	1253524	1253524	35
637799663	'Synpcc7942_1234'	'+'	Chromosome	1254739	7.8	1254540	1254524	1254516	1254512	1254512	1254517	1254520	219
637799675	'Synpcc7942_1246'	'+'	Chromosome	1270803	1.8	1270640	1270663	1270661	1270660	1270660	1270660	1270657	146
637799692	'Synpcc7942_1262'	'-'	Chromosome	1286647	2.0	1286735	1286673	1286750	1286735	1286735	1286749	1286730	83
637799701	'Synpcc7942_1271'	'-'	Chromosome	1296175	2.0	1296144	1296215	1296202	1296208	1296208	1296204	1296197	22
637799715	'Synpcc7942_1285'	'-'	Chromosome	1307200	2.0	1307359	1307274	1307277	1307275	1307275	1307275	1307289	89
637799720	'Synpcc7942_1290'	'-'	Chromosome	1313460	4.1	1313499	1313503	1313503	1313502	1313502	1313504	1313502	42
637799723	'Synpcc7942_1293'	'-'	Chromosome	1318598	1.9	1318899	1318643	1318643	1318899	1318899	1318692	1318779	181
637799729	'Synpcc7942_1299'	'-'	Chromosome	1327854	2.2	1327916	1327882	1327956	1327913	1327913	1327955	1327923	69
637799731	'Synpcc7942_1301'	'+'	Chromosome	1328678	4.6	1328664	1328683	1328691	1328692	1328692	1328663	1328681	-3
637799758	'Synpcc7942_1327'	'+'	Chromosome	1360808	3.2	1360754	1360755	1360757	1360757	1360757	1360736	1360753	55
637799767	'Synpcc7942_1336'	'+'	Chromosome	1367261	5.9	1367090	1367076	1367046	1367073	1367073	1367073	1367072	189
637799770	'Synpcc7942_1339'	'-'	Chromosome	1373973	1.8	1373924	1373997	1374004	1374002	1374002	1374004	1373989	16
637799772	'Synpcc7942_1341'	'+'	Chromosome	1374756	2.7	1374667	1374614	1374498	1374615	1374615	1374663	1374612	144
637799785	'Synpcc7942_1354'	'+'	Chromosome	1386587	31.8	1386406	1386408	1386408	1386412	1386412	1386638	1386447	140
637799803	'Synpcc7942_1371'	'-'	Chromosome	1409368	4.1	1409407	1409398	1409398	1409438	1409438	1409422	1409417	49
637799814	'Synpcc7942_1382'	'+'	Chromosome	1427042	2.0	1426921	1426927	1426865	1426947	1426947	1426955	1426927	115
637799828	'Synpcc7942_1396'	'-'	Chromosome	1446000	4.6	1446139	1446143	1446140	1446140	1446140	1446143	1446141	141
637799829	'Synpcc7942_1397'	'+'	Chromosome	1446191	2.7	1446139	1446143	1446140	1446140	1446140	1446143	1446141	50
637799833	'Synpcc7942_1401'	'-'	Chromosome	1453104	1.8	1453149	1453134	1453142	1453132	1453132	1453150	1453140	36
637799834	'Synpcc7942_1402'	'+'	Chromosome	1453317	4.6	1453149	1453134	1453142	1453132	1453132	1453150	1453140	177
637799837	'Synpcc7942_1405'	'+'	Chromosome	1456260	3.4	1456221	1456209	1456208	1456204	1456204	1456178	1456204	56
637799839	'Synpcc7942_1407'	'+'	Chromosome	1458057	1.8	1457954	1457962	1457964	1457961	1457961	1457960	1457960	97
637799843	'Synpcc7942_1411'	'-'	Chromosome	1464358	2.5	1464378	1464371	1464387	1464373	1464373	1464383	1464378	20
637799844	'Synpcc7942_1412'	'-'	Chromosome	1464817	2.3	1464870	1464870	1464869	1464871	1464871	1464869	1464870	53
637799846	'Synpcc7942_1414'	'-'	Chromosome	1466434	1.8	1466493	1466479	1466735	1466479	1466479	1466473	1466523	89

Supplementary Table 1 (Continued).

637799848	'Synpcc7942_1416'	'+'	Chromosome	1468344	2.7	1468212	1468202	1468223	1468192	1468192	1468174	1468199	145
637799856	'Synpcc7942_1424'	'+'	Chromosome	1477713	2.3	1477497	1477459	1477461	1477462	1477462	1477464	1477468	245
637799857	'Synpcc7942_1425'	'+'	Chromosome	1478240	1.8	1478202	1478204	1478207	1478205	1478205	1478205	1478205	35
637799858	'Synpcc7942_1426'	'+'	Chromosome	1479461	2.3	1479301	1479299	1479301	1479300	1479300	1479300	1479300	161
637799878	'Synpcc7942_1446'	'-'	Chromosome	1500342	2.3	1500459	1500460	1500469	1500465	1500465	1500463	1500464	122
637799879	'Synpcc7942_1447'	'+'	Chromosome	1500489	1.9	1500459	1500460	1500469	1500465	1500465	1500463	1500464	25
637799898	'Synpcc7942_1466'	'+'	Chromosome	1519664	1.9	1519669	1519671	1519672	1519672	1519672	1519672	1519671	-7
637799913	'Synpcc7942_1481'	'-'	Chromosome	1532398	2.4	1532444	1532438	1532420	1532428	1532428	1532434	1532432	34
637799914	'Synpcc7942_1482'	'+'	Chromosome	1532605	1.8	1532444	1532438	1532420	1532428	1532428	1532434	1532432	173
637799918	'Synpcc7942_1486'	'-'	Chromosome	1536912	2.0	1536953	1536954	1536954	1536956	1536956	1536955	1536955	43
637799930	'Synpcc7942_1497'	'-'	Chromosome	1548105	2.7	1548137	1548136	1548134	1548128	1548128	1548130	1548132	27
637799932	'Synpcc7942_1499'	'-'	Chromosome	1548930	2.2	1548991	1548998	1548997	1548998	1548998	1548999	1548997	67
637799937	'Synpcc7942_1504'	'+'	Chromosome	1553330	3.2	1553287	1553282	1553246	1553293	1553293	1553306	1553285	45
637799939	'Synpcc7942_1506'	'-'	Chromosome	1556513	4.2	1556569	1556569	1556567	1556567	1556567	1556567	1556568	55
637799941	'Synpcc7942_1508'	'-'	Chromosome	1559209	2.0	1559304	1559300	1559300	1559302	1559302	1559299	1559301	92
637799942	'Synpcc7942_1509'	'+'	Chromosome	1559329	2.1	1559304	1559300	1559300	1559302	1559302	1559299	1559301	28
637799946	'Synpcc7942_1513'	'+'	Chromosome	1563532	1.8	1563418	1563415	1563416	1563416	1563416	1563416	1563416	116
637799950	'Synpcc7942_1517'	'-'	Chromosome	1568316	2.0	1568389	1568388	1568387	1568384	1568384	1568391	1568387	71
637799951	'Synpcc7942_1518'	'+'	Chromosome	1568627	1.9	1568389	1568388	1568387	1568384	1568384	1568391	1568387	240
637799958	'Synpcc7942_1525'	'+'	Chromosome	1583407	2.1	1583194	1583195	1583195	1583319	1583319	1583326	1583258	149
637799962	'Synpcc7942_1529'	'+'	Chromosome	1589204	2.0	1589180	1589169	1589171	1589166	1589166	1589166	1589170	34
637799982	'Synpcc7942_1549'	'+'	Chromosome	1606129	1.8	1605924	1605830	1605830	1605964	1605964	1605963	1605913	216
637799984	'Synpcc7942_1551'	'+'	Chromosome	1608052	2.1	1607755	1608103	1607767	1607753	1607753	1607753	1607814	238
637799989	'Synpcc7942_1556'	'+'	Chromosome	1612870	6.5	1612836	1612835	1612841	1612836	1612836	1612837	1612837	33
637799990	'Synpcc7942_1557'	'-'	Chromosome	1614396	7.1	1614546	1614539	1614541	1614541	1614541	1614543	1614542	146
637800000	'Synpcc7942_1567'	'-'	Chromosome	1626019	13.7	1626019	1626048	1626048	1626001	1626001	1625970	1626015	-4
637800016	'Synpcc7942_1583'	'+'	Chromosome	1648210	2.2	1648154	1648163	1648165	1648167	1648167	1648191	1648168	42
637800046	'Synpcc7942_1612'	'-'	Chromosome	1681905	83.8	1682016	1682014	1682017	1682016	1682016	1682016	1682016	111
637800052	'Synpcc7942_1616'	'+'	Chromosome	1683163	2.3	1682864	1683132	1683134	1683132	1683132	1683128	1683087	76
637800053	'Synpcc7942_1617'	'+'	Chromosome	1683752	1.8	1683726	1683712	1683713	1683713	1683713	1683712	1683715	37
637800074	'Synpcc7942_1637'	'-'	Chromosome	1706484	2.2	1706655	1706646	1706652	1706651	1706651	1706652	1706651	167
637800080	'Synpcc7942_1643'	'+'	Chromosome	1710353	1.9	1710290	1710271	1710293	1710293	1710293	1710300	1710290	63
637800081	'Synpcc7942_1644'	'+'	Chromosome	1712014	2.7	1711888	1711891	1711891	1711891	1711891	1711891	1711891	123
637800083	'Synpcc7942_1646'	'+'	Chromosome	1714348	3.8	1714182	1714192	1714222	1714187	1714187	1714147	1714186	162
637800093	'Synpcc7942_1656'	'-'	Chromosome	1728081	3.6	1728251	1728251	1728249	1728250	1728250	1728260	1728252	171
637800098	'Synpcc7942_1661'	'+'	Chromosome	1731159	39.4	1730960	1731033	1730960	1730958	1730958	1730955	1730971	188
637800102	'Synpcc7942_1664'	'+'	Chromosome	1733790	2.1	1733698	1733696	1733698	1733700	1733700	1733701	1733699	91
637800106	'Synpcc7942_1668'	'+'	Chromosome	1737882	10.3	1737771	1737767	1737813	1737821	1737821	1737781	1737796	86

Supplementary Table 1 (Continued).

637800108	'Synpcc7942_1670'	'+'	Chromosome	1741687	Inf	1741536	1741695	1741611	1741713	1741713	1741704	1741662	25
637800109	'Synpcc7942_1671'	'+'	Chromosome	1741836	5.3	1741537	1741746	1741611	1741713	1741713	1741704	1741671	165
637800138	'Synpcc7942_1700'	'-'	Chromosome	1767849	1.8	1767933	1767927	1767928	1767928	1767928	1767928	1767929	80
637800139	'Synpcc7942_1701'	'+'	Chromosome	1767953	2.0	1767933	1767927	1767928	1767928	1767928	1767928	1767929	24
637800154	'Synpcc7942_1716'	'-'	Chromosome	1787655	1.8	1787711	1787729	1787754	1787755	1787755	1787693	1787733	78
637800158	'Synpcc7942_1719'	'-'	Chromosome	1791796	2.3	1791837	1791839	1791836	1791835	1791835	1791837	1791837	41
637800184	'Synpcc7942_1745'	'-'	Chromosome	1816393	1.9	1816402	1816404	1816423	1816413	1816413	1816407	1816410	17
637800197	'Synpcc7942_1756'	'-'	Chromosome	1824511	12.0	1824646	1824654	1824656	1824656	1824656	1824656	1824654	143
637800198	'Synpcc7942_1757'	'+'	Chromosome	1824648	15.2	1824646	1824654	1824656	1824656	1824656	1824656	1824654	-6
637800201	'Synpcc7942_1760'	'+'	Chromosome	1826528	2.1	1826442	1826446	1826442	1826445	1826445	1826446	1826444	84
637800209	'Synpcc7942_1768'	'+'	Chromosome	1835596	1.8	1835458	1835438	1835499	1835463	1835463	1835503	1835471	125
637800217	'Synpcc7942_1776'	'+'	Chromosome	1840742	2.4	1840724	1840722	1840722	1840721	1840721	1840722	1840722	20
637800224	'Synpcc7942_1783'	'+'	Chromosome	1849303	3.3	1849086	1849159	1849158	1849158	1849158	1849156	1849146	157
637800225	'Synpcc7942_1784'	'+'	Chromosome	1852529	11.0	1852468	1852450	1852450	1852452	1852452	1852473	1852458	71
637800240	'Synpcc7942_1799'	'+'	Chromosome	1868940	4.3	1868856	1868859	1868856	1868858	1868858	1868859	1868858	82
637800245	'Synpcc7942_1804'	'-'	Chromosome	1874397	3.0	1874469	1874440	1874432	1874440	1874440	1874433	1874442	45
637800267	'Synpcc7942_1826'	'-'	Chromosome	1897163	1.8	1897231	1897253	1897257	1897251	1897251	1897258	1897250	87
637800271	'Synpcc7942_1830'	'-'	Chromosome	1899550	2.3	1899628	1899589	1899589	1899627	1899627	1899716	1899629	79
637800272	'Synpcc7942_1831'	'-'	Chromosome	1901019	2.0	1901032	1901042	1901043	1901042	1901042	1901043	1901041	22
637800273	'Synpcc7942_1832'	'-'	Chromosome	1901601	2.0	1901750	1901747	1901750	1901747	1901747	1901746	1901748	147
637800279	'Synpcc7942_1838'	'-'	Chromosome	1905957	9.4	1906010	1906015	1906015	1906015	1906015	1906015	1906014	57
637800290	'Synpcc7942_1849'	'+'	Chromosome	1916620	181.6	1916533	1916531	1916535	1916533	1916533	1916321	1916498	122
637800306	'Synpcc7942_1865'	'+'	Chromosome	1935472	2.5	1935457	1935444	1935444	1935445	1935445	1935444	1935447	25
637800337	'Synpcc7942_1896'	'-'	Chromosome	1969898	3.0	1969920	1969921	1969921	1969920	1969920	1969923	1969921	23
637800356	'Synpcc7942_1914'	'+'	Chromosome	1990394	2.1	1990352	1990362	1990362	1990363	1990363	1990365	1990361	33
637800363	'Synpcc7942_1921'	'+'	Chromosome	1998203	3.0	1998188	1998190	1998191	1998190	1998190	1998190	1998190	13
637800386	'Synpcc7942_1944'	'+'	Chromosome	2018389	1.9	2018326	2018328	2018329	2018328	2018328	2018329	2018328	61
637800392	'Synpcc7942_1949'	'+'	Chromosome	2024003	3.2	2023978	2023977	2023977	2023976	2023976	2023987	2023979	24
637800393	'Synpcc7942_1950'	'+'	Chromosome	2024388	4.1	2024089	2024089	2024089	2024089	2024089	2024439	2024147	241
637800403	'Synpcc7942_1960'	'-'	Chromosome	2032696	6.2	2032722	2032728	2032729	2032731	2032731	2032734	2032729	33
637800421	'Synpcc7942_1976'	'-'	Chromosome	2047397	2.8	2047426	2047427	2047426	2047426	2047426	2047426	2047426	29
637800432	'Synpcc7942_1987'	'+'	Chromosome	2057819	2.7	2057788	2057788	2057789	2057787	2057787	2057783	2057787	32
637800438	'Synpcc7942_1993'	'+'	Chromosome	2063554	2.4	2063605	2063558	2063526	2063533	2063533	2063598	2063559	-5
637800447	'Synpcc7942_2002'	'+'	Chromosome	2071335	2.3	2071305	2071306	2071308	2071308	2071308	2071304	2071307	28
637800457	'Synpcc7942_2012'	'+'	Chromosome	2081506	1.8	2081428	2081427	2081426	2081425	2081425	2081425	2081426	80
637800471	'Synpcc7942_2026'	'+'	Chromosome	2094451	2.3	2094443	2094411	2094417	2094412	2094412	2094414	2094418	33
637800478	'Synpcc7942_2033'	'+'	Chromosome	2102330	1.8	2102326	2102300	2102301	2102282	2102282	2102304	2102299	31
637800486	'Synpcc7942_2041'	'+'	Chromosome	2110181	1.8	2110182	2110227	2110171	2110165	2110165	2110182	2110182	-1

Supplementary Table 1 (Continued).

637800488	'Synpcc7942_2043'	'-'	Chromosome	2112672	2.1	2112892	2112899	2112904	2112903	2112903	2112904	2112901	229
637800495	'Synpcc7942_2050'	'+'	Chromosome	2126401	1.8	2126286	2126277	2126278	2126279	2126279	2126279	2126280	121
637800498	'Synpcc7942_2053'	'+'	Chromosome	2130328	3.2	2130255	2130310	2130303	2130304	2130304	2130352	2130305	23
637800504	'Synpcc7942_2059'	'-'	Chromosome	2137272	2.1	2137356	2137364	2137363	2137363	2137363	2137362	2137362	90
637800524	'Synpcc7942_2079'	'-'	Chromosome	2157755	8.5	2158049	2157889	2157890	2158056	2158056	2158056	2157999	244
637800525	'Synpcc7942_2080'	'+'	Chromosome	2158038	3.7	2158089	2157889	2157890	2158089	2158089	2158089	2158023	15
637800527	'Synpcc7942_2082'	'-'	Chromosome	2163575	11.1	2163700	2163700	2163702	2163702	2163702	2163700	2163701	126
637800528	'Synpcc7942_2083'	'+'	Chromosome	2163925	3.0	2163700	2163700	2163702	2163702	2163702	2163700	2163701	224
637800541	'Synpcc7942_2096'	'+'	Chromosome	2177467	2.1	2177383	2177385	2177386	2177386	2177386	2177384	2177385	82
637800547	'Synpcc7942_2102'	'+'	Chromosome	2183837	2.8	2183837	2183837	2183832	2183787	2183787	2183787	2183811	26
637800548	'Synpcc7942_2103'	'-'	Chromosome	2184523	3.3	2184565	2184558	2184556	2184558	2184558	2184580	2184563	40
637800554	'Synpcc7942_2109'	'+'	Chromosome	2189141	2.2	2189087	2189091	2189098	2189092	2189092	2189094	2189092	49
637800579	'Synpcc7942_2134'	'-'	Chromosome	2214708	1.8	2214790	2214796	2214789	2214791	2214791	2214795	2214792	84
637800594	'Synpcc7942_2149'	'+'	Chromosome	2231897	1.9	2231918	2231883	2231840	2231878	2231878	2231839	2231873	24
637800605	'Synpcc7942_2160'	'+'	Chromosome	2242713	2.0	2242680	2242683	2242674	2242682	2242682	2242677	2242680	33
637800607	'Synpcc7942_2162'	'-'	Chromosome	2244940	9.0	2244998	2245010	2245013	2245012	2245012	2245011	2245009	69
637800622	'Synpcc7942_2177'	'+'	Chromosome	2257143	2.1	2257129	2257130	2257131	2257132	2257132	2257132	2257131	12
637800623	'Synpcc7942_2178'	'-'	Chromosome	2258395	2.7	2258400	2258417	2258687	2258419	2258419	2258416	2258460	65
637800630	'Synpcc7942_2185'	'+'	Chromosome	2263403	10.7	2263376	2263375	2263378	2263376	2263376	2263450	2263389	14
637800632	'Synpcc7942_2187'	'-'	Chromosome	2266102	1.8	2266270	2266270	2266273	2266275	2266275	2266272	2266273	171
637800645	'Synpcc7942_2200'	'-'	Chromosome	2281077	2.6	2281301	2281299	2281299	2281299	2281299	2281301	2281300	223
637800688	'Synpcc7942_2241'	'+'	Chromosome	2306546	1.8	2306581	2306581	2306580	2306583	2306583	2306248	2306526	20
637800695	'Synpcc7942_2248'	'-'	Chromosome	2315727	2.5	2315754	2315757	2315755	2315755	2315755	2315754	2315755	28
637800700	'Synpcc7942_2253'	'-'	Chromosome	2323299	2.5	2323304	2323312	2323303	2323304	2323304	2323299	2323304	5
637800708	'Synpcc7942_2261'	'-'	Chromosome	2329790	1.9	2329801	2329881	2329881	2329880	2329880	2329881	2329867	77
637800714	'Synpcc7942_2267'	'+'	Chromosome	2335846	23.9	2335800	2335818	2335820	2335816	2335816	2335816	2335814	32
637800726	'Synpcc7942_2279'	'+'	Chromosome	2347614	7.2	2347495	2347529	2347530	2347542	2347542	2347527	2347528	86
637800727	'Synpcc7942_2280'	'-'	Chromosome	2350167	2.0	2350288	2350294	2350302	2350291	2350291	2350318	2350297	130
637800738	'Synpcc7942_2291'	'-'	Chromosome	2361251	2.1	2361237	2361261	2361264	2361261	2361261	2361270	2361259	8
637800745	'Synpcc7942_2297'	'-'	Chromosome	2368721	4.7	2368760	2368757	2368757	2368757	2368757	2368757	2368758	37
637800746	'Synpcc7942_2298'	'+'	Chromosome	2368966	3.0	2368760	2368757	2368757	2368757	2368757	2368757	2368758	208
637800749	'Synpcc7942_2301'	'+'	Chromosome	2370542	2.4	2370453	2370508	2370517	2370457	2370457	2370506	2370483	59
637800754	'Synpcc7942_2306'	'+'	Chromosome	2374134	6.4	2374111	2374108	2374108	2374109	2374109	2374109	2374109	25
637800757	'Synpcc7942_2309'	'-'	Chromosome	2377703	2.9	2377767	2377768	2377764	2377763	2377763	2377764	2377765	62
637800763	'Synpcc7942_2315'	'+'	Chromosome	2383870	2.2	2383787	2383706	2383742	2383787	2383787	2383793	2383767	103
637800774	'Synpcc7942_2326'	'+'	Chromosome	2393509	49.0	2393489	2393488	2393488	2393488	2393488	2393492	2393489	20
637800783	'Synpcc7942_2335'	'-'	Chromosome	2403955	17.6	2404001	2403993	2403992	2403993	2403993	2403996	2403995	40
637800784	'Synpcc7942_2336'	'-'	Chromosome	2404389	34.5	2404458	2404456	2404456	2404456	2404456	2404458	2404457	68

Supplementary Table 1 (Continued).

637800788	'Synpcc7942_2340'	'+'	Chromosome	2407881	2.1	2407859	2407859	2407860	2407858	2407858	2407861	2407859	22
637800794	'Synpcc7942_2346'	'+'	Chromosome	2413356	2.6	2413268	2413266	2413263	2413265	2413265	2413263	2413265	91
637800800	'Synpcc7942_2352'	'-'	Chromosome	2420198	2.5	2420286	2420287	2420289	2420294	2420294	2420287	2420290	92
637800832	'Synpcc7942_2384'	'+'	Chromosome	2451384	14.1	2451358	2451356	2451356	2451356	2451356	2451356	2451356	28
637800834	'Synpcc7942_2386'	'+'	Chromosome	2455998	7.1	2455853	2455832	2455815	2455828	2455828	2455830	2455831	167
637800836	'Synpcc7942_2388'	'-'	Chromosome	2460331	19.5	2460395	2460395	2460392	2460395	2460395	2460390	2460394	63
637800839	'Synpcc7942_2391'	'+'	Chromosome	2465228	3.6	2465146	2465175	2465224	2465164	2465164	2465162	2465173	55
637800852	'Synpcc7942_2404'	'+'	Chromosome	2477807	2.4	2477508	2477766	2477771	2477765	2477765	2477737	2477719	88
637800860	'Synpcc7942_2412'	'-'	Chromosome	2485251	2.2	2485243	2485211	2485211	2485336	2485336	2485332	2485278	27
637800874	'Synpcc7942_2426'	'-'	Chromosome	2498893	1.8	2498993	2498976	2498990	2498984	2498984	2498972	2498983	90
637800880	'Synpcc7942_2432'	'+'	Chromosome	2506121	4.0	2506084	2506062	2506123	2505822	2505822	2505822	2505956	165
637800895	'Synpcc7942_2447'	'+'	Chromosome	2524094	2.5	2523943	2523946	2523947	2523948	2523948	2523946	2523946	148
637800897	'Synpcc7942_2449'	'+'	Chromosome	2526169	2.5	2526128	2526127	2526130	2526130	2526130	2526130	2526129	40
637800902	'Synpcc7942_2454'	'-'	Chromosome	2533374	2.0	2533494	2533493	2533496	2533495	2533495	2533455	2533488	114
637800907	'Synpcc7942_2458'	'+'	Chromosome	2536184	2.5	2536104	2536154	2536158	2536159	2536159	2536151	2536148	36
637800910	'Synpcc7942_2461'	'-'	Chromosome	2542737	30.6	2542827	2542789	2542790	2542791	2542791	2542759	2542791	54
637800935	'Synpcc7942_2486'	'-'	Chromosome	2568305	3.0	2568336	2568338	2568338	2568337	2568337	2568339	2568338	33
637800948	'Synpcc7942_2499'	'-'	Chromosome	2581055	2.9	2581344	2581026	2581040	2581047	2581047	2581237	2581124	69
637800949	'Synpcc7942_2500'	'-'	Chromosome	2581716	3.1	2581889	2581867	2581868	2581890	2581890	2581894	2581883	167
637800953	'Synpcc7942_2504'	'-'	Chromosome	2586072	1.9	2586105	2586100	2586103	2586103	2586103	2586104	2586103	31
637800956	'Synpcc7942_2507'	'-'	Chromosome	2587797	3.0	2587794	2587825	2587824	2587797	2587797	2587824	2587810	13
637800965	'Synpcc7942_2516'	'-'	Chromosome	2596958	2.6	2596909	2596930	2596986	2596925	2596925	2596977	2596942	-16
637800971	'Synpcc7942_2522'	'-'	Chromosome	2605010	3.0	2605142	2605143	2605139	2605135	2605135	2605134	2605138	128
637800976	'Synpcc7942_2527'	'+'	Chromosome	2608875	2.2	2608796	2608823	2608769	2608811	2608811	2608809	2608803	72
637800985	'Synpcc7942_2535'	'+'	Chromosome	2615811	2.8	2615666	2615860	2615859	2615569	2615569	2615567	2615682	129
637800996	'Synpcc7942_2546'	'+'	Chromosome	2626237	1.9	2626213	2626223	2626220	2626222	2626222	2626214	2626219	18
637801004	'Synpcc7942_2554'	'-'	Chromosome	2633647	4.1	2633682	2633681	2633680	2633681	2633681	2633681	2633681	34
637801005	'Synpcc7942_2555'	'-'	Chromosome	2635086	10.3	2635152	2635105	2635101	2635091	2635091	2635099	2635107	21
637801007	'Synpcc7942_2557'	'-'	Chromosome	2636354	16.7	2636404	2636406	2636404	2636406	2636406	2636415	2636407	53
637801016	'Synpcc7942_2566'	'+'	Chromosome	2645522	1.9	2645447	2645436	2645442	2645442	2645442	2645439	2645441	81
637801020	'Synpcc7942_2570'	'-'	Chromosome	2650032	2.2	2650029	2650060	2650050	2650058	2650058	2650052	2650051	19
637801029	'Synpcc7942_2576'	'-'	Chromosome	2662110	1.8	2662157	2662177	2662167	2662177	2662177	2662165	2662170	60
637801044	'Synpcc7942_2590'	'+'	Chromosome	2674093	184.0	2674063	2674066	2674066	2674067	2674067	2674062	2674065	28
637801056	'Synpcc7942_2602'	'+'	Chromosome	2684044	3.8	2683933	2683956	2683933	2684013	2684013	2683919	2683961	83
637801063	'Synpcc7942_2609'	'+'	Chromosome	2691626	2.3	2691599	2691600	2691604	2691606	2691606	2691602	2691603	23
637801067	'Synpcc7942_2613'	'-'	Chromosome	2695870	3.5	2695903	2695903	2695903	2695903	2695903	2695903	2695903	33
637800185	'Synpcc7942_1746'	'-'	Chromosome	1817562	1.5	1817716	1817681	1817658	1817691	1817691	1817699	1817689	127

Supplementary Table 2. RpoD6 genomic binding sites determined by analysis of time-course ChIP-seq datasets that are proximal to transcription start sites of high confidence circadian genes.

Supplementary Table 2 (Continued).

Information for high-confidence circadian transcript whose 5'TSS is located in proximity to RpoD6 binding		Genomic location of RpoD6 binding site	Determination of maximum enrichment relative to mock within interval of each RpoD6 binding site											
JGI ID	Synpcc_7942 number		T=24h	T=28h	T=32h	T=36h	T=40h	T=44h	T=48h	T=52h	T=56h	T=60h	T=64h	T=68h
637798428	'Synpcc7942_0023'	24563	3.8	6.7	1.5	1.6	1.5	1.1	1.9	8.3	3.3	1.9	1.9	3.2
637798444	'Synpcc7942_0039'	36828	2.3	4.4	1.1	1.3	1.4	1.0	1.8	5.6	4.2	1.6	1.0	2.4
637798496	'Synpcc7942_0090'	88149	20.6	27.6	6.7	9.9	6.8	8.6	14.2	27.8	25.5	8.8	4.4	13.8
637798506	'Synpcc7942_0100'	101173	1.7	2.5	1.9	1.4	1.2	0.6	1.1	6.0	2.0	0.8	0.8	2.1
637798650	'Synpcc7942_0244'	241546	8.5	10.7	1.1	2.2	1.4	1.9	7.8	12.4	14.6	3.1	1.4	4.9
637798658	'Synpcc7942_0252'	248415	2.1	3.5	0.7	0.9	0.9	0.7	1.2	3.2	2.9	1.3	0.7	1.6
637798684	'Synpcc7942_0278'	273533	4.7	5.2	1.0	1.8	2.0	0.9	2.6	7.0	5.8	1.4	1.8	3.0
637798685	'Synpcc7942_0279'	273533	3.5	4.5	1.2	1.2	1.5	0.9	2.0	5.2	4.3	1.7	1.3	2.4
637798697	'Synpcc7942_0291'	288270	4.2	6.5	2.5	2.6	2.4	1.1	2.0	10.8	4.6	2.4	1.6	3.2
637798711	'Synpcc7942_0305'	303818	1.2	2.1	3.5	3.0	2.7	1.0	0.6	9.6	1.3	1.1	1.1	2.0
637798737	'Synpcc7942_0331'	327422	7.0	8.4	3.0	3.3	3.8	2.9	2.0	11.3	2.2	4.0	3.2	5.4
637798742	'Synpcc7942_0336'	330785	3.9	5.6	1.3	1.5	1.5	1.4	1.5	3.7	3.0	1.2	2.1	3.3
637798744	'Synpcc7942_0338'	333254	6.1	6.3	1.1	1.7	1.1	1.6	3.1	6.6	6.7	2.6	1.1	2.6
637798757	'Synpcc7942_0351'	343565	7.0	10.4	2.9	3.3	2.5	1.9	4.3	13.1	9.0	2.6	2.1	4.7
637798784	'Synpcc7942_0378'	372160	2.1	2.2	1.1	1.1	0.8	0.7	1.0	4.2	1.2	0.9	0.8	1.8
637798794	'Synpcc7942_0388'	382450	2.7	3.9	0.9	0.9	1.0	0.8	1.7	4.4	3.5	1.1	0.7	2.3
637798889	'Synpcc7942_0482'	469218	5.0	6.0	2.6	1.7	2.0	1.2	3.7	8.8	4.9	1.8	1.5	3.9
637798892	'Synpcc7942_0485'	470982	8.5	10.4	2.3	3.5	3.1	2.5	6.5	13.5	10.6	3.7	2.3	6.2
637798906	'Synpcc7942_0499'	488719	3.5	5.8	0.9	1.0	1.3	1.0	2.5	6.0	6.2	1.4	0.8	2.4
637798912	'Synpcc7942_0505'	493166	8.9	14.1	3.1	3.9	3.6	3.1	7.8	14.4	13.1	4.4	3.2	6.9
637798964	'Synpcc7942_0556'	539384	2.4	4.1	3.0	2.8	1.9	0.8	2.0	10.6	3.6	2.0	1.3	2.2
637798977	'Synpcc7942_0569'	551819	3.1	3.5	7.0	4.3	4.4	1.6	2.7	15.8	3.4	1.8	3.5	3.7
637799006	'Synpcc7942_0595'	583412	7.5	11.2	2.8	2.3	2.0	2.2	5.5	13.0	12.9	3.0	2.2	4.7
637799020	'Synpcc7942_0609'	596408	12.4	16.3	4.2	5.7	4.1	2.7	9.2	17.9	13.7	4.1	4.3	9.4
637799051	'Synpcc7942_0639'	630568	9.2	16.3	7.2	7.4	6.3	3.3	3.7	32.1	7.8	7.2	4.3	8.6
637799059	'Synpcc7942_0647'	640780	3.3	3.7	0.7	1.3	1.3	1.2	1.5	4.2	2.5	1.6	0.9	2.5
637799061	'Synpcc7942_0649'	644127	2.2	2.4	2.0	1.9	1.5	0.7	0.7	8.3	0.8	1.7	1.3	1.9
637799391	'Synpcc7942_0972'	978893	1.7	4.0	0.6	0.2	0.7	1.0	2.6	3.5	5.2	0.9	0.8	2.8
637799464	'Synpcc7942_1042'	1055621	6.0	4.8	8.2	5.5	3.0	1.5	2.2	18.0	4.0	2.1	3.1	4.0
637799479	'Synpcc7942_1057'	1067467	5.5	7.3	2.1	2.6	1.9	1.3	3.0	9.4	5.8	2.9	1.7	3.6
637799497	'Synpcc7942_1072'	1084625	6.8	8.4	2.0	1.4	1.7	2.0	8.0	11.6	16.1	1.8	2.5	4.4
637799499	'Synpcc7942_1074'	1085895	6.1	9.3	1.9	2.4	1.5	1.3	5.3	8.5	11.0	1.8	1.3	3.4
637799522	'Synpcc7942_1096'	1114841	2.2	3.0	0.4	1.5	1.0	0.7	1.4	3.9	3.2	1.2	0.5	1.2
637799534	'Synpcc7942_1108'	1124939	1.8	2.0	0.6	0.8	0.8	0.3	2.0	3.3	3.4	0.3	0.4	1.0

Supplementary Table 2 (Continued).

637799582	'Synpcc7942_1156'	1183345	2.4	3.5	3.7	7.7	6.4	0.7	1.3	14.7	3.2	4.6	1.6	1.2
637799655	'Synpcc7942_1226'	1247018	3.6	6.3	2.7	2.8	2.3	1.2	1.9	10.1	2.9	2.7	1.6	3.1
637799659	'Synpcc7942_1230'	1252161	1.9	3.5	0.5	0.5	0.5	0.5	2.1	1.9	4.1	0.5	0.4	1.1
637799701	'Synpcc7942_1271'	1296322	1.3	3.1	1.3	0.7	0.1	0.6	1.2	3.1	2.5	0.9	0.2	1.4
637799715	'Synpcc7942_1285'	1307513	2.4	4.4	0.4	1.0	0.9	0.4	3.2	3.9	6.0	0.9	0.8	1.8
637799723	'Synpcc7942_1293'	1318738	2.0	3.3	1.0	1.1	1.0	0.5	1.3	4.3	2.9	1.2	0.8	1.8
637799828	'Synpcc7942_1396'	1446146	6.1	11.6	10.4	8.9	7.9	2.5	3.8	34.0	2.9	6.7	4.4	7.9
637799829	'Synpcc7942_1397'	1446146	6.0	11.3	10.1	8.7	7.7	2.4	3.7	33.0	2.8	6.5	4.3	7.7
637799918	'Synpcc7942_1486'	1536952	6.3	12.0	7.6	9.5	6.6	2.2	2.6	39.2	5.4	6.9	3.2	6.9
637799930	'Synpcc7942_1497'	1548053	3.6	4.5	0.8	1.8	1.3	0.8	2.0	5.7	3.8	1.7	0.8	1.8
637799950	'Synpcc7942_1517'	1568868	3.8	4.3	0.7	0.9	0.7	0.7	3.1	5.0	7.3	1.5	1.0	2.8
637799989	'Synpcc7942_1556'	1612856	1.8	2.5	0.8	2.0	1.8	0.3	1.0	6.8	2.0	2.1	0.7	1.1
637799990	'Synpcc7942_1557'	1614443	4.1	4.0	11.1	8.4	8.6	3.4	3.6	22.1	4.2	3.5	4.1	4.2
637800052	'Synpcc7942_1616'	1682635	10.0	18.5	11.8	14.6	9.7	4.6	5.5	48.2	9.7	9.7	6.6	12.6
637800197	'Synpcc7942_1756'	1824737	1.1	1.4	2.5	3.2	1.9	0.5	1.0	5.7	1.8	0.9	0.4	0.8
637800245	'Synpcc7942_1804'	1874364	2.4	4.0	8.3	4.5	3.7	1.3	2.3	13.4	2.6	2.0	2.9	1.9
637800271	'Synpcc7942_1830'	1899585	2.2	2.0	6.3	6.6	5.8	1.3	1.7	18.3	2.7	3.4	2.6	2.9
637800272	'Synpcc7942_1831'	1901046	8.1	16.3	9.6	9.9	6.8	3.5	4.4	42.0	7.7	8.1	5.4	11.8
637800273	'Synpcc7942_1832'	1901749	3.4	4.5	5.4	4.2	3.6	1.4	2.0	16.5	2.4	2.5	2.2	3.8
637800279	'Synpcc7942_1838'	1906006	1.1	2.6	0.6	1.7	1.6	0.4	1.1	3.5	2.9	1.5	0.8	0.8
637800290	'Synpcc7942_1849'	1916081	3.1	4.1	2.6	3.1	2.9	1.2	1.0	12.0	1.3	2.8	2.0	3.1
637800363	'Synpcc7942_1921'	1998207	16.7	31.0	10.4	13.7	8.2	4.4	8.8	53.8	18.4	11.6	8.3	18.4
637800432	'Synpcc7942_1987'	2057816	4.1	3.4	6.9	6.1	5.3	1.7	2.6	22.4	2.0	3.7	2.9	3.9
637800457	'Synpcc7942_2012'	2081435	7.8	12.6	5.9	4.0	3.5	1.8	4.0	22.8	6.8	3.9	3.4	6.9
637800495	'Synpcc7942_2050'	2126191	3.9	4.8	2.5	2.4	2.2	1.5	1.6	10.9	1.5	2.7	2.0	4.1
637800504	'Synpcc7942_2059'	2137361	1.6	2.2	3.5	2.0	1.7	0.8	1.2	10.6	2.1	1.2	1.2	2.3
637800645	'Synpcc7942_2200'	2281300	6.3	10.4	5.9	7.6	5.8	2.2	2.3	24.7	3.3	6.1	3.9	6.0
637800714	'Synpcc7942_2267'	2335826	6.0	8.8	7.3	12.8	9.5	1.3	5.6	30.6	9.4	9.4	2.2	3.5
637800763	'Synpcc7942_2315'	2383681	6.4	11.1	6.6	8.8	2.7	2.3	1.7	29.2	5.8	5.5	2.5	7.8
637800788	'Synpcc7942_2340'	2407858	2.5	4.2	1.9	2.2	1.5	1.0	1.5	8.0	2.3	1.9	1.3	2.6
637800794	'Synpcc7942_2346'	2413262	12.5	22.8	13.7	16.0	13.0	5.3	5.3	55.9	7.0	13.9	8.4	13.3
637800800	'Synpcc7942_2352'	2420361	2.7	3.3	3.9	3.2	3.3	1.1	2.2	11.6	1.8	1.6	1.9	2.8
637800902	'Synpcc7942_2454'	2533456	7.7	12.3	6.1	5.8	4.6	2.3	4.4	26.0	7.8	5.7	3.8	6.7
637800971	'Synpcc7942_2522'	2605142	2.1	4.8	5.0	8.0	6.3	1.1	1.1	20.5	3.4	5.9	2.3	3.3
637801016	'Synpcc7942_2566'	2645497	4.5	6.3	2.0	2.3	1.9	1.0	2.3	8.7	4.2	2.7	1.7	3.7

Supplementary Table 3. RpoD5 genomic binding sites determined by analysis of time-course ChIP-seq datasets that are proximal to transcription start sites of high confidence circadian genes.

Supplementary Table 3. (Continued).

Information for high-confidence circadian transcript whose 5'TSS is located in proximity to RpoD5 binding		Genomic location of RpoD5 binding site	Determination of maximum enrichment relative to mock within interval of each RpoD5 binding site											
JGI ID	Synpcc_7942 number		T=24h	T=28h	T=32h	T=36h	T=40h	T=44h	T=48h	T=52h	T=56h	T=60h	T=64h	T=68h
637798409	'Synpcc7942_0004'	4192	2.1	2.5	1.6	10.5	4.5	2.1	0.9	4.3	3.2	13.8	1.9	2.3
637798425	'Synpcc7942_0020'	20469	2.3	2.1	2.2	15.8	4.2	2.0	1.1	5.0	3.4	14.9	1.8	1.4
637798431	'Synpcc7942_0026'	28386	1.6	2.4	1.9	10.3	4.4	1.8	0.9	4.0	2.5	11.3	1.9	1.9
637798444	'Synpcc7942_0039'	36836	2.0	1.7	1.2	3.3	3.5	1.4	1.1	3.1	1.8	6.7	1.4	1.5
637798492	'Synpcc7942_0086'	85313	0.7	1.4	0.9	3.4	2.8	1.3	0.4	2.2	1.8	5.6	0.9	1.0
637798496	'Synpcc7942_0090'	88272	7.4	10.7	7.1	30.1	23.1	7.8	2.7	16.0	9.8	56.0	8.5	6.8
637798579	'Synpcc7942_0173'	173308	0.7	0.8	0.8	6.6	1.9	0.7	0.4	2.0	1.0	6.3	1.0	1.0
637798650	'Synpcc7942_0244'	241614	2.3	3.3	3.4	23.6	6.3	2.2	0.9	5.9	4.5	24.3	3.8	2.4
637798651	'Synpcc7942_0245'	242764	1.5	1.7	1.6	1.4	3.7	1.2	1.5	1.9	1.5	3.5	1.5	1.4
637798658	'Synpcc7942_0252'	248402	1.2	1.0	1.2	2.8	2.2	0.9	0.5	2.1	1.6	5.3	1.5	1.2
637798697	'Synpcc7942_0291'	287846	1.5	1.7	2.9	4.1	3.6	2.5	0.7	3.3	5.1	9.9	1.7	2.0
637798722	'Synpcc7942_0316'	315008	1.0	1.3	1.8	4.5	2.4	1.2	0.7	2.3	2.1	6.9	1.4	0.7
637798744	'Synpcc7942_0338'	333266	2.2	3.0	1.5	6.3	5.5	2.0	1.1	4.0	3.4	12.7	2.5	4.0
637798757	'Synpcc7942_0351'	343566	2.4	2.1	2.8	9.4	5.6	2.5	0.9	5.6	3.7	16.1	2.3	2.6
637798775	'Synpcc7942_0369'	361740	1.7	1.9	1.6	13.3	4.2	2.1	1.1	3.4	2.1	12.2	2.3	2.0
637798776	'Synpcc7942_0370'	363612	9.1	7.5	6.5	28.6	18.6	9.7	5.6	17.3	11.1	49.1	9.4	7.9
637798797	'Synpcc7942_0391'	385526	1.0	1.5	1.1	13.0	3.9	0.9	0.8	3.5	2.0	11.3	1.9	1.3
637798817	'Synpcc7942_0411'	403262	2.7	5.1	4.0	9.4	11.1	5.0	3.5	8.5	6.0	20.1	4.8	5.0
637798889	'Synpcc7942_0482'	469166	1.7	2.0	1.8	7.5	4.5	1.9	1.7	3.4	3.1	9.3	2.1	2.0
637798890	'Synpcc7942_0483'	469771	2.0	2.4	1.8	15.8	6.0	2.5	1.8	4.5	3.0	14.7	2.2	2.2
637798912	'Synpcc7942_0505'	493204	3.7	5.2	2.7	20.8	8.6	3.4	2.4	7.7	4.6	23.8	4.4	2.7
637798952	'Synpcc7942_0544'	526627	1.6	1.5	1.0	8.3	4.4	1.7	0.7	3.8	2.2	10.2	1.8	1.9
637798964	'Synpcc7942_0556'	539560	0.9	1.1	1.3	4.5	2.3	0.7	0.5	1.9	1.4	5.3	1.2	0.8
637798977	'Synpcc7942_0569'	552043	0.8	1.2	0.7	2.8	2.5	1.2	0.9	2.0	1.1	5.6	1.2	0.9
637798981	'Synpcc7942_0573'	555961	1.6	2.1	1.6	4.5	4.1	1.8	1.4	3.1	3.1	9.5	1.8	1.3
637799006	'Synpcc7942_0595'	583784	2.7	3.6	1.5	16.6	6.6	3.0	1.6	8.5	4.7	20.7	3.0	1.9
637799080	'Synpcc7942_0668'	664625	0.5	0.9	0.5	3.8	1.7	0.6	0.8	1.3	0.9	4.0	1.0	0.6
637799082	'Synpcc7942_0670'	664625	1.4	1.7	1.1	10.9	4.8	1.0	1.0	3.7	2.4	11.4	1.5	1.8
637799084	'Synpcc7942_0672'	666482	0.5	0.4	0.5	4.7	1.2	0.5	0.3	1.6	0.9	4.2	0.7	0.7
637799115	'Synpcc7942_0703'	694030	8.3	11.0	5.8	35.0	27.9	11.5	6.0	23.8	18.7	65.8	12.8	9.2
637799171	'Synpcc7942_0756'	749937	1.8	3.5	0.9	23.1	6.4	1.6	0.7	6.2	1.8	21.3	1.9	1.3
637799196	'Synpcc7942_0780'	774560	1.6	2.3	1.7	11.7	6.2	2.0	1.1	5.5	2.8	17.3	1.8	1.7
637799205	'Synpcc7942_0789'	785538	2.8	2.3	2.0	12.3	2.8	2.3	1.5	3.0	3.3	12.1	3.2	2.0
637799212	'Synpcc7942_0796'	790702	1.6	2.6	2.4	12.3	5.8	2.7	2.5	6.6	3.9	16.9	2.5	2.8

Supplementary Table 3. (Continued).

637799213	'Synpcc7942_0797'	791550	1.4	1.9	2.5	14.2	4.0	1.6	0.9	4.8	2.5	13.3	1.8	1.3
637799245	'Synpcc7942_0828'	823707	1.1	0.8	1.0	4.4	1.5	1.1	0.5	1.8	1.2	5.5	0.8	0.8
637799252	'Synpcc7942_0836'	832617	0.9	1.2	0.8	7.5	2.9	0.7	0.1	2.8	1.1	7.8	1.1	1.5
637799277	'Synpcc7942_0861'	865793	1.8	2.2	8.7	5.2	1.0	2.8	1.7	5.7	12.7	1.1	3.5	1.5
637799278	'Synpcc7942_0862'	865195	1.7	1.8	5.0	4.3	4.2	1.6	1.2	3.3	7.4	5.9	2.0	1.0
637799391	'Synpcc7942_0972'	978918	0.8	0.8	0.8	5.0	3.2	0.9	0.5	3.9	1.1	7.9	0.8	0.8
637799412	'Synpcc7942_0993'	1003508	0.5	1.0	0.8	10.2	3.2	1.0	0.1	2.5	1.4	9.5	1.2	0.9
637799430	'Synpcc7942_1010'	1022859	0.6	1.1	2.2	10.9	2.9	1.0	0.2	4.4	3.9	8.8	1.3	0.7
637799439	'Synpcc7942_1019'	1032770	0.4	0.5	0.3	5.4	1.8	0.4	0.4	1.9	1.3	6.6	0.6	0.7
637799479	'Synpcc7942_1057'	1067201	1.8	2.2	2.8	10.3	4.3	2.0	1.2	4.5	5.0	9.3	2.3	2.3
637799497	'Synpcc7942_1072'	1084625	0.9	1.6	1.2	28.3	6.7	1.6	0.6	6.5	1.9	24.8	2.3	2.4
637799534	'Synpcc7942_1108'	1124848	0.5	0.6	0.5	5.8	2.0	0.4	0.4	1.6	0.9	5.3	0.5	0.8
637799585	'Synpcc7942_1159'	1193788	0.1	0.3	0.2	3.0	1.4	0.1	0.0	1.2	0.4	4.9	-0.1	0.4
637799656	'Synpcc7942_1227'	1249456	1.7	1.9	1.4	5.1	5.1	2.1	0.7	4.0	2.3	14.0	1.4	1.4
637799659	'Synpcc7942_1230'	1252173	0.9	0.6	0.4	4.8	2.0	0.8	0.4	1.7	0.5	6.0	0.6	0.8
637799715	'Synpcc7942_1285'	1307520	1.3	1.4	0.8	11.8	3.1	0.8	0.1	3.2	1.8	10.8	0.6	1.3
637799723	'Synpcc7942_1293'	1318860	1.0	1.1	1.1	2.7	2.3	0.8	0.5	1.8	1.5	5.1	1.1	0.9
637799758	'Synpcc7942_1327'	1360396	0.8	1.3	0.9	4.1	2.8	0.7	1.0	4.0	2.1	10.9	1.2	0.9
637799828	'Synpcc7942_1396'	1446045	1.3	1.5	3.7	4.3	0.3	1.0	1.3	4.1	6.7	1.7	1.7	0.6
637799829	'Synpcc7942_1397'	1445870	1.0	1.3	3.6	4.2	1.6	0.9	0.7	4.0	6.5	2.8	1.7	0.6
637799857	'Synpcc7942_1425'	1478021	2.1	1.5	0.9	7.0	4.0	1.9	0.8	3.3	3.1	10.8	1.7	2.0
637799913	'Synpcc7942_1481'	1532745	1.8	2.4	1.8	12.5	4.4	2.0	0.9	3.8	2.2	11.3	2.4	2.2
637799950	'Synpcc7942_1517'	1568833	0.9	1.5	1.0	11.0	3.5	1.2	0.4	3.5	1.9	11.3	1.7	0.7
637799951	'Synpcc7942_1518'	1568149	1.3	0.9	0.7	3.1	3.8	1.6	0.4	3.4	1.6	7.9	1.7	1.3
637800052	'Synpcc7942_1616'	1682841	1.4	1.8	2.8	7.7	3.0	1.3	0.9	3.8	4.4	5.6	2.1	1.2
637800138	'Synpcc7942_1700'	1768227	1.1	1.3	0.8	7.5	3.0	1.2	0.8	4.2	1.9	10.2	0.9	1.2
637800184	'Synpcc7942_1745'	1816642	1.6	2.4	2.4	6.7	5.8	1.5	2.2	5.0	2.2	16.2	2.3	2.7
637800197	'Synpcc7942_1756'	1825155	0.6	1.0	0.7	2.8	1.2	0.6	0.6	1.6	1.4	3.2	0.9	0.4
637800267	'Synpcc7942_1826'	1897682	3.7	7.5	4.8	41.6	14.7	5.3	3.5	13.8	11.2	43.0	9.9	5.0
637800290	'Synpcc7942_1849'	1916136	5.9	6.0	6.9	6.8	6.8	5.5	3.9	6.1	10.8	3.6	6.4	5.2
637800356	'Synpcc7942_1914'	1990072	1.9	2.8	1.5	3.3	3.9	2.3	3.0	2.3	2.6	5.1	3.3	2.5
637800432	'Synpcc7942_1987'	2057288	0.7	0.8	2.3	4.0	1.5	0.5	0.8	1.6	3.2	1.6	1.6	0.7
637800438	'Synpcc7942_1993'	2063164	1.3	1.9	2.2	11.6	3.4	1.4	0.4	3.7	3.4	13.3	1.8	1.4
637800488	'Synpcc7942_2043'	2113260	1.4	1.9	1.1	17.6	4.1	2.0	0.7	3.4	2.5	13.3	2.1	1.9
637800495	'Synpcc7942_2050'	2126136	2.4	2.6	1.7	2.1	4.2	2.4	2.0	2.0	2.9	2.9	2.7	2.7
637800504	'Synpcc7942_2059'	2137688	0.4	0.7	1.3	3.2	1.4	0.5	0.3	1.2	1.6	3.6	0.7	0.4
637800688	'Synpcc7942_2241'	2306627	1.5	1.8	1.3	6.0	4.4	2.3	1.3	3.7	2.8	9.0	1.6	1.8
637800700	'Synpcc7942_2253'	2323468	1.1	1.3	1.8	3.8	3.1	1.5	0.8	2.8	2.7	6.7	1.4	1.1

Supplementary Table 3. (Continued).

637800708	'Synpcc7942_2261'	2330176	1.2	1.5	1.3	12.1	4.6	1.8	0.8	3.1	2.1	10.5	1.8	1.5
637800738	'Synpcc7942_2291'	2361508	1.0	1.7	1.0	4.5	3.0	1.4	0.4	2.6	2.3	7.5	1.6	1.3
637800788	'Synpcc7942_2340'	2407666	0.9	1.0	3.3	4.1	1.5	1.0	0.4	3.9	5.7	4.2	1.4	0.9
637800794	'Synpcc7942_2346'	2413366	1.4	1.6	4.8	5.0	1.4	1.2	0.8	5.1	7.8	2.8	2.3	1.3
637800800	'Synpcc7942_2352'	2420517	0.7	1.1	4.5	7.1	1.2	0.5	0.5	4.3	6.1	2.6	2.2	0.6
637800839	'Synpcc7942_2391'	2464844	1.2	1.5	0.8	7.6	3.4	0.9	0.4	3.0	1.7	8.7	1.4	1.3
637800880	'Synpcc7942_2432'	2505762	1.3	1.6	1.0	5.4	2.7	1.3	0.9	3.0	2.2	6.2	1.5	1.3
637800895	'Synpcc7942_2447'	2523758	1.6	2.5	1.4	9.5	5.0	2.6	2.0	4.4	3.4	14.7	1.7	2.1
637800902	'Synpcc7942_2454'	2533591	2.0	3.0	5.1	12.8	4.7	2.4	1.5	7.6	8.2	9.7	2.9	2.5
637800948	'Synpcc7942_2499'	2581366	0.7	1.5	1.1	5.5	2.6	0.8	0.8	2.3	1.8	6.8	0.9	1.1
637800971	'Synpcc7942_2522'	2605639	0.6	0.7	2.2	2.4	1.2	0.6	0.7	2.1	3.7	2.0	1.1	0.6
637800976	'Synpcc7942_2527'	2608637	0.8	1.3	0.7	2.8	2.5	1.1	0.5	2.4	1.7	5.1	1.1	0.8
637801005	'Synpcc7942_2555'	2635257	2.4	3.4	2.0	23.6	6.5	2.1	1.3	7.3	2.8	20.8	2.6	2.2
637801007	'Synpcc7942_2557'	2636713	0.9	1.7	1.6	7.2	3.4	1.8	0.5	4.2	3.4	9.0	2.3	1.5
637801020	'Synpcc7942_2570'	2650179	1.3	2.1	1.8	5.7	4.0	1.5	0.9	4.3	3.3	9.7	2.0	1.8
637801029	'Synpcc7942_2576'	2662511	2.8	3.8	3.9	24.7	10.3	4.6	2.4	8.6	5.1	25.9	2.9	2.7
637801063	'Synpcc7942_2609'	2691291	2.1	2.7	1.6	2.8	5.6	2.9	1.8	3.5	3.7	5.5	2.7	2.8

Supplementary Table 4. SigF2 genomic binding sites determined by analysis of time-course ChIP-seq datasets that are proximal to transcription start sites of high confidence circadian genes

Information for high-confidence circadian transcript whose 5'TSS is located in proximity to SigF2 binding		Genomic location of RpoD5 binding site	Determination of maximum enrichment relative to mock within interval of each SigF2 binding site											
JGI ID	Synpcc_7942 number		T=24h	T=28h	T=32h	T=36h	T=40h	T=44h	T=48h	T=52h	T=56h	T=60h	T=64h	T=68h
637798710	'Synpcc7942_0304'	302675	3.2	2.9	2.9	3.2	10.8	4.8	2.5	5.4	3.9	3.6	5.4	4.8
637798737	'Synpcc7942_0331'	327576	6.2	4.3	3.6	4.5	12.9	5.8	5.8	5.3	4.5	4.1	6.9	5.3
637798775	'Synpcc7942_0369'	361918	3.1	2.6	2.3	2.2	7.6	2.6	2.4	3.0	2.2	2.9	3.5	3.0
637798889	'Synpcc7942_0482'	469111	1.9	2.4	2.0	2.4	7.0	3.9	2.3	2.4	2.6	3.5	4.2	2.9
637798890	'Synpcc7942_0483'	469475	2.7	3.0	1.9	2.7	9.7	4.0	2.4	3.2	2.8	3.6	5.3	3.3
637798892	'Synpcc7942_0485'	470461	4.2	5.2	3.8	4.3	19.4	6.8	3.6	6.8	4.5	5.6	7.5	6.8
637799020	'Synpcc7942_0609'	596397	5.2	5.6	5.1	5.4	27.7	11.0	4.2	8.5	5.5	8.5	11.8	8.2
637799051	'Synpcc7942_0639'	630610	2.4	2.8	3.8	2.3	10.6	5.1	2.8	3.7	3.2	4.2	4.7	4.7
637799115	'Synpcc7942_0703'	694045	19.1	20.6	28.7	16.1	55.9	37.1	19.2	25.5	29.8	25.5	43.6	19.1
637799205	'Synpcc7942_0789'	785790	4.8	4.8	3.8	4.6	12.1	5.3	5.1	4.9	4.9	4.3	6.4	5.7
637799391	'Synpcc7942_0972'	978833	1.6	1.9	1.8	2.4	8.6	4.3	1.0	2.0	1.8	3.6	6.0	2.8
637799839	'Synpcc7942_1407'	1457867	2.6	1.0	1.2	2.3	7.0	1.2	2.0	1.9	1.7	1.9	2.1	3.2
637800225	'Synpcc7942_1784'	1852485	8.3	4.7	8.4	5.1	11.0	8.9	7.0	6.7	8.5	5.5	11.1	4.3
637800630	'Synpcc7942_2185'	2263071	2.1	2.7	2.3	2.9	8.1	3.0	1.4	3.2	2.1	2.8	3.8	2.7
637800727	'Synpcc7942_2280'	2350462	2.2	1.5	1.3	2.0	7.6	3.4	1.9	2.2	2.0	3.1	4.3	2.5
637800852	'Synpcc7942_2404'	2477355	5.4	3.8	3.6	4.6	11.7	4.9	4.2	4.0	3.7	4.6	6.6	4.1
637801004	'Synpcc7942_2554'	2633681	3.4	2.3	4.2	2.5	3.9	6.5	2.0	2.4	4.3	2.6	8.9	2.1